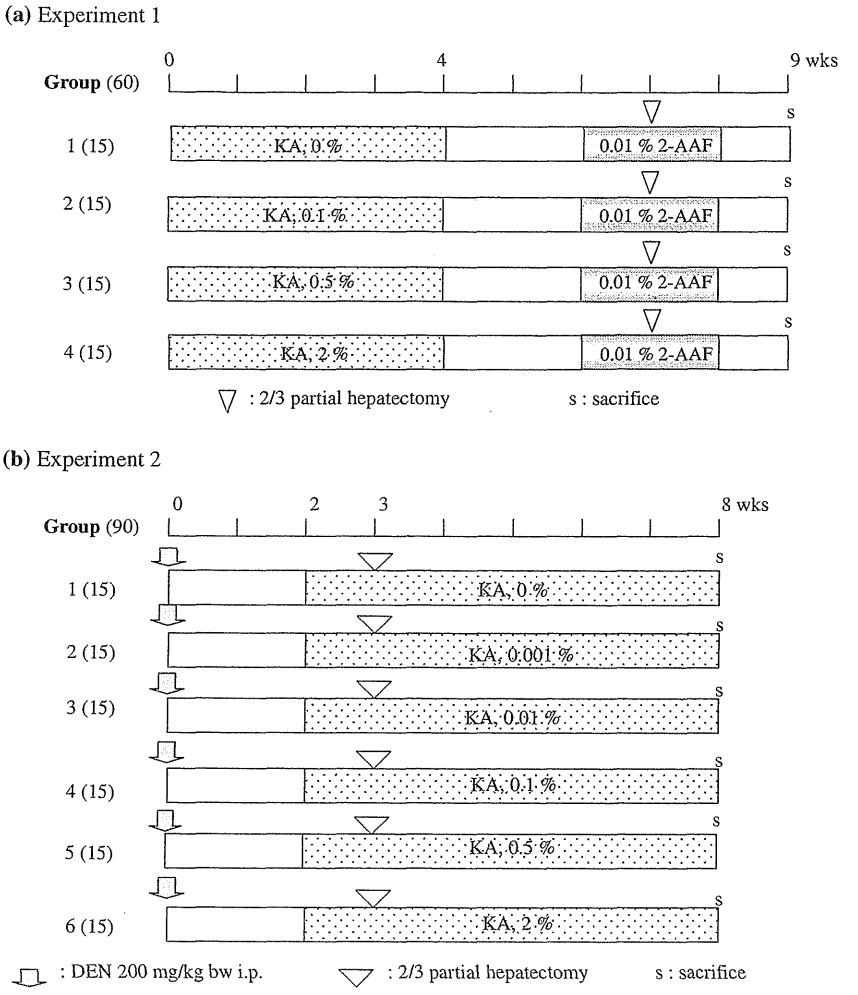

Fig. 1. Scheme of experimental designs.

hepatocarcinogenesis, and 2 weeks after that the rats were administered a diet containing KA 0%, 0.001%, 0.01%, 0.1%, 0.5% and 2% for 6 weeks. Animals were subjected to two-thirds partial hepatectomy at week 3 (Ito et al., 1989, 2003; Takada et al., 1994). The total observation period was 8 weeks.

All surviving animals were killed at the end of these experiments, their livers were removed and weighed, and then 2–3 mm thick sections from three lobes were fixed in formalin and embedded in paraffin wax. Sections cut at 4 μm were used for histopathological and immunohistochemical examination. The remaining liver tissue was preserved in liquid nitrogen.

These experiments were done under the guidelines of the animal facility of Osaka City University Medical School.

2.4. Immunohistochemistry for GST-P positive foci

The avidin–biotin peroxidase complex method (Vectastain ABC kit, Vector Lab.) was used to demonstrate the GST-P positive liver foci, a putative preneoplastic lesion. An immunohistochemical analysis was carried out with sequential treatments of rabbit anti-rat GST-P (1:2000) as a primary antibody, goat anti-rabbit IgG antibody as a secondary antibody, and the peroxidase-antiperoxidase complex. For final visualization of the GST-P positive foci, those that were larger than 0.2 mm in diameter were counted. The total area of liver sections was measured using an Image Processor for Analytical Pathology (IPAP; Sumica Technos, Osaka, Japan) to give values per cm^2 of liver section.

2.5. Immunohistochemistry for proliferation cell nuclear antigen (PCNA) and double immunohistochemistry for PCNA and GST-P

In experiment 1, PCNA staining was performed using an anti-PCNA mouse monoclonal antibody (1:500). After deparaffinizing with xylene, alcohol and distilled water, endogenous peroxidase was blocked with 3% hydrogen peroxide (H_2O_2) for 5 min. The sections were then treated in a microwave oven in a solution of 0.1 mM citrate buffer pH 6.0 for 15 min and then transferred to distilled water. After rinsing in phosphate buffer saline (PBS), the sections were incubated with normal horse serum in PBS for 15 min. For detection of PCNA, the sections were incubated with anti-PCNA mouse monoclonal antibody at 37 °C for 1 h and then incubated with anti-mouse IgG antibody as a secondary antibody for 30 min at room temperature. Color was developed with diaminobenzidine tetrachloride (DAB). Finally, the sections were counterstained with haematoxylin, dehydrated and placed on a cover slide. The PCNA indices were counted as the number of positive nuclei per 1000 hepatocytes.

In experiment 2, double staining for PCNA and GST-P positive foci was performed using the same method as described before. After developing color with DAB, the sections were washed in running tap water and Tris–HCl–phosphate buffer saline (TBS). For GST-P detection, the sections were blocked for unspecific binding with normal goat serum in TBS for 15 min and then incubated with rabbit anti-rat GST-P antibody at 1:2000 dilutions as the primary antibody at 37 °C for 1 h. After that, the sections were incubated

Table 1
Final body weight, liver weights and food and water consumption of rats treated with various concentrations of KA (experiment 1).

Treatment	No. of rat examined	Final body weight (g)	Food consumption (g/rat/day)	Water consumption (g/rat/day)	Liver weight	
					Absolute (g)	Relative (%)
0% KA	15	249.7 ± 10.1	13.0 ± 3.8	18.2 ± 3.3	5.76 ± 0.73	2.31 ± 0.29
0.1% KA	15	265.7 ± 11.5*	13.5 ± 3.9	18.7 ± 3.6	6.66 ± 0.79*	2.51 ± 0.29
0.5% KA	14	267.8 ± 10.6*	13.2 ± 3.1	18.7 ± 3.4	6.73 ± 1.40*	2.50 ± 0.47
2% KA	15	247.1 ± 11.1	11.1 ± 2.7	16.7 ± 2.5	6.12 ± 0.49	2.48 ± 0.17

* Significantly different from control group (DEN alone) at $p < 0.05$.

with DAKO Envision labelled polymer-AP (mouse/rabbit) for 30 min and color developed with DAKO New Fuchin Substrate System. Finally, the sections were counterstained with haematoxylin and mounted with Aquatex. The PCNA indices were estimated for GST-P positive areas as numbers of positive nuclei per 1000 cells.

2.6. Measurement of 8-OHdG levels in DNA

DNA samples were isolated from pieces of frozen liver weighing 500 mg using DNA Extractor WB kit (Wako Pure Chemical Industries Ltd., Osaka, Japan), containing sodium iodide (NaI), deferoxamine mesylate (Sigma Chemical Co., St. Louis, MO) and RNase (Wako Pure Chemical Industries Ltd., Osaka, Japan), then digested into deoxynucleosides by combined treatment with nuclease P1 and alkaline phosphatase. Finally the samples were filtered using an Ultrafree-MC 100,000NMWL filter unit (Millipore Co., Bedford, MA). The level of 8-OHdG in each resultant preparation was determined by HPLC-ECD using a Beckman Coulter Ultrasphere Ods column 4.6 mm × 25 cm which controlled the temperature at 35 °C, flow rate 1 ml/min, L2D2 lamp and Esa Coulochem II electrochemical detector. The level of 8-OHdG formation was expressed as the number of 8-OHdG residues/10^5 total deoxyguanosines.

2.7. Immunohistochemistry for apoptosis

Immunohistochemistry for apoptosis (TUNEL) were performed using an ApopTag Peroxidase *in situ* kit (Chemicon International Inc., Germany). After deparaffinization, the sections were pretreated with proteinase K (20 μg/ml) and endogenous peroxidase quenched with 3% H_2O_2. Then, the sections were enzymatically added to terminal deoxynucleotidyl transferase (TdT) and labeled with the digoxigenin-nucleotide. After that, they were allowed to bind with an anti-digoxigenin antibody that was conjugated to a peroxidase reporter molecule. Finally, the bound peroxidase antibody was conjugated enzymatically and generated color from a chromogenic substrate. The apoptotic index is assessed as apoptotic bodies per 1000 hepatocytes.

2.8. Statistical analysis

All results are presented as mean ± SD. All of the statistical analyses were carried out by Dunnett's multiple comparison tests. Statistical significance was evaluated at $p < 0.05$.

3. Results

3.1. Experiment 1: liver initiation assay

Final body weight and absolute liver weights were significantly increased in the group administered the KA at concentrations of 0.1% and 0.5% as compared with the values for the control groups, but there were no significant differences among the groups with regard to food and water consumption (Table 1). No change in liver/body weight ratio was induced by the administration of KA at various concentrations as compared with the control group. The food and water intake of the 2% KA fed group were slightly less than those of the other groups due to the KA treatment. Rat's appetite became normal after cessation of KA feeding.

Table 2
GST-P positive foci and 8-OHdG level of rats treated with various concentrations of KA (experiment 1) (diameter ⩾ 0.2 mm) (mean ± SD).

Treatment	No. of rat examined	GST-P positive foci		8-OHdG level (8-OHdG/10^5 dG)
		Number (No./cm^2)	Area (mm^2/cm^2)	
0% KA	15	2.67 ± 1.07	0.15 ± 0.08	0.16 ± 0.02
0.1% KA	15	2.13 ± 0.47	0.13 ± 0.07	0.14 ± 0.01
0.5% KA	14	2.84 ± 0.77	0.16 ± 0.09	0.17 ± 0.04
2% KA	15	3.69 ± 1.53	0.18 ± 0.09	0.20 ± 0.05

Data on the effect of various concentrations of KA on formation of GST-P positive foci in the liver are shown in Table 2. Two percent KA slightly increased GST-P positive foci in the number ($p = 0.074$) and area ($p = 0.554$) of GST-P positive foci formation compared with non-treated groups, but there was no significant difference. Furthermore, there were no remarkable differences between KA-treated and non-treated groups in 8-OHdG formation levels in rat liver DNA (Table 2). PCNA positive index and apoptotic index did not change among groups (data not shown).

3.2. Experiment 2: liver promotion assay

Data on the effect of KA application at different concentrations by body weight and liver weight after DEN-initiation are shown in Table 3. There were no significant differences among the groups with regards to food and water consumption. After 6 weeks of continuous KA administration to rats initiated with DEN, the 2% KA treatment significantly increased absolute and relative liver weights but slightly decreased final rat body weight (Table 3).

In 2% KA-treated rats, the numbers and areas of GST-P positive foci were markedly increased, while 0.001–0.5% KA treatment had no effect on GST-P positive foci formation compared with a control group (Fig. 2). Histological examination found that high concentration of KA induced centrilobular hypertrophy, eosinophilic focus, basophilic focus and mixed cell focus, which were all correlated with GST-P positive foci in rat livers. The 2% KA-treated group also showed a significantly increased PCNA positive index in the GST-P area (Table 4). HPLC analysis revealed 8-OHdG levels in rat livers to be significantly increased in the group fed with 0.5% and 2% KA. Analysis via the TUNEL assay demonstrated significant increases of apoptosis in the livers of rats treated with 0.01% and 0.1% KA, but not in those treated with 0.5% and 2% after DEN initiation.

4. Discussion

In the present study, we examined the initiation activity of KA in a medium-term liver initiation assay using partially hepatectomized rats. The many indicators assessed, including GST-P positive foci, widely recognized to be hepatocellular preneoplastic lesions,

Table 3
Final body weight, liver weights and food and water consumption of rats treated with various concentrations of KA after DEN-initiation (experiment 2).

Treatment	No. of rats examined	Body weight (g)	Food consumption (g/rat/day)	Water consumption (g/rat/day)	Liver weight	
					Absolute (g)	Relative (%)
DEN	15	240.4 ± 15.0	12.4 ± 2.6	18.2 ± 1.7	7.06 ± 0.38	2.97 ± 0.12
DEN + 0.001% KA	13	250.4 ± 6.3	12.4 ± 3.1	18.4 ± 2.2	7.40 ± 0.38	2.96 ± 0.13
DEN + 0.01% KA	15	251.7 ± 14.7	12.2 ± 2.6	18.7 ± 1.6	7.19 ± 0.47	2.85 ± 0.14
DEN + 0.1% KA	15	254.5 ± 8.6	12.2 ± 2.7	18.2 ± 1.7	6.68 ± 0.95	2.67 ± 0.18
DEN + 0.5% KA	15	246.5 ± 7.6	12.2 ± 3.1	17.8 ± 2.1	7.58 ± 0.41	3.02 ± 0.08
DEN + 2% KA	14	227.5 ± 8.9	11.1 ± 2.5	16.8 ± 2.0	7.90 ± 0.49*	3.46 ± 0.21*

* Significantly different from control group (DEN alone) at $p < 0.05$.

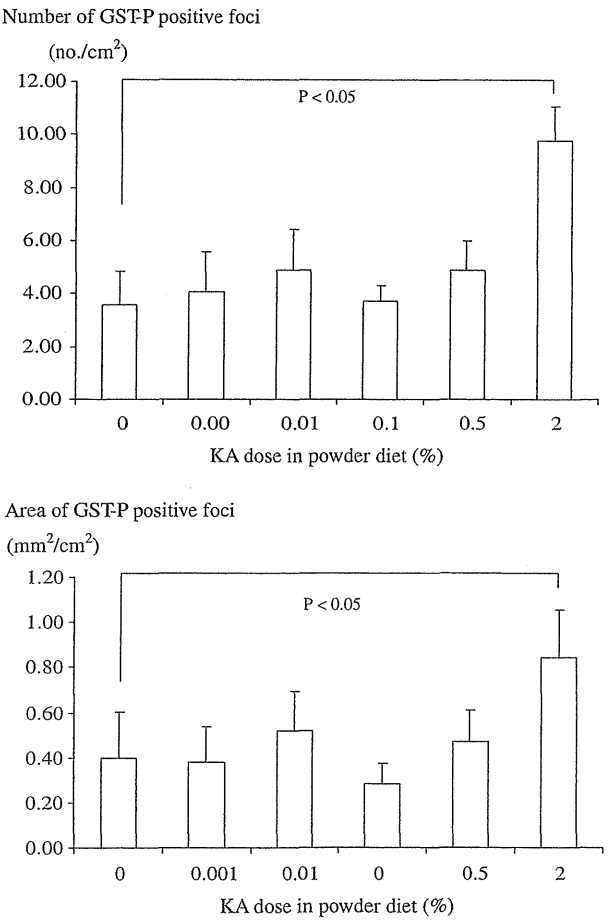

Fig. 2. Number and area of GST-P positive liver cell foci in partially hepatectomized rat treated with various concentrations of KA after DEN initiation (Experiment 2). Data represent the mean ± SD.

8-OHdG formation, cell proliferation and apoptotic index, were not significantly different in the groups treated with various concentrations of KA compared to the control groups. Although there were body weight changes during the experiment, these results showed no relation with the other carcinogenesis biomarkers. Even though there were body weight decreases in the 2% KA-treated group during the KA treatment period, these returned to normal in the final stages after cessation of KA feeding. The same results were observed by Higa et al. (2007). On the other hand, the body weight of low concentrations of KA treated rats significantly increased. This may be partly due to the influence of KA on thyroid hormones which regulate rat basal metabolism (Fujimoto et al., 1999; Bray et al., 1976). From previous studies, it is still unclear whether KA is a genotoxic or non-genotoxic carcinogen. The genotoxic profile of KA has been reported as positive in (1) Ames assay either with or without metabolic activation at high concentration of KA; (2) sister chromatid exchange and chromosome aberration in CHO cells (Wei et al., 1991); and (3) induced thyroid-proliferative lesions in rodents (Fujimoto et al., 1998; Mitsumori et al., 1999; Moto et al., 2006). These studies contradict the negative results from rat hepatocyte unscheduled DNA synthesis and bone marrow micronucleus tests (Nohynek et al., 2004), and lack of initiating activity on rodent hepatocarcinogenesis (Watanabe et al., 2005; Moto et al., 2006). In our study for initiation activity, the induction of GST-P positive foci in the rat livers did not show any significant difference. In addition, 8-OHdG formation level was also found not to differ from that of the control group. Therefore, we conclude that KA does not have any initiation activity on rat hepatocarcinogenesis.

To investigate the promoting activity on rat hepatocarcinogenesis, DEN was used as an initiator following administering to rats of various concentrations of KA in the diet, and in parallel with partial hepatectomy. The data demonstrated that only high concentration (2%) of KA significantly induced the number and area of GST-P positive foci formation. These results agree with those of Takizawa and his colleagues (Takizawa et al., 2004). Furthermore, our studies suggest that the low concentration (0.001%) of KA in the daily intake of humans should have no adverse effects. Moreover, the experiment showed no effect on GST-P positive foci formation at low and medium concentrations (0.01–0.5 %). 8-OHdG formation levels significantly increased with KA at concentrations of 0.5% and 2%, and cell proliferation was significantly increased at a concentration of 2%. Thus, KA increasing GST-P formation with a high concentration of KA might be involved with oxidative stress induc-

Table 4
PCNA positive index, 8-OHdG level and apoptotic index of rats treated with various concentrations of KA after DEN-initiation (experiment 2).

Treatment	No. of rats examined	PCNA positive index (No./1000 hepatocyte)	8-OHdG level (per 10^5 dG)	Apoptotic index (No./1000 hepatocyte)
DEN	15	19.68 ± 1.87	0.37 ± 0.07	14.00 ± 1.86
DEN + 0.001% KA	13	17.49 ± 0.54	0.46 ± 0.06	11.91 ± 1.58
DEN + 0.01% KA	15	16.99 ± 3.45	0.41 ± 0.08	20.56 ± 4.71*
DEN + 0.1% KA	15	16.44 ± 2.92	0.39 ± 0.06	26.57 ± 4.60*
DEN + 0.5% KA	15	20.96 ± 1.33	0.58 ± 0.08*	14.20 ± 2.34
DEN + 2% KA	14	24.10 ± 1.46*	0.57 ± 0.04*	12.88 ± 3.19

* Significantly different from control group (DEN alone) at $p < 0.05$.

tion and increased cell proliferation, while there are no effects on apoptotic pathways. These findings may indicate that KA exerts a promoting activity of rat hepatocarcinogenesis at high concentration, but not at low, showing the existence of a threshold in KA carcinogenicity. This corresponds to the observations of Umemura et al. (1999) that pentachlorophenol (PCP) induces promotion but does not initiate heaptocarcinogenesis in B6C3F1 mice livers.

In another study we examined the effect of KA on xenobiotic metabolizing enzyme (P450) via a short term study. Briefly, rats were given KA by oral administration at various concentrations for 2 weeks and then the livers were analyzed for hepatic P450 levels in various isozymes using Western blot analysis. Doses of 2% KA significantly increased CYP2B1 level (unpublished data). Klaunig and Kamendulis (2004) proposed that reactive oxygen species (ROS), such as superoxide anions, or hydrogen peroxide and hydroxyl radicals, can be produced from several sources during metabolism by cytochrome P450. Similarly, metabolism of Phenobarbital by CYP2B is involved in the oxygenation and uncoupling of catalytic activation and subsequent release of superoxide anions. In addition, the ROS can react with DNA to form oxidative DNA damage, 8-OHdG – which is a marker of cellular oxidative stress during carcinogenesis (Kasai, 1997). Thus, KA treatment at high doses in the promotion stage induced overexpression of P450, such as CYP2B1. This may contribute to an increase of 8-OHdG formation through ROS, which then promotes an increase of cell proliferation and finally increases induction of GST-P positive foci. Thus, the induction of oxidative stress has an important role for KA hepatocarcinogenesis in rats. Biochemical processes are capable of repairing the DNA damage. Since, in experiment 1, liver samples measured for 8-OHdG formation were obtained 5 weeks after cessation of KA treatment, the formation levels would not be different among the various groups.

KA carcinogenicity in rat livers has a non-genotoxic mode of action; we observed no initiation activity but did find positive promotion activity. Moreover, since the promotion activity was exerted only at high concentration (2% KA), the carcinogenic effect of KA will not occur up to a certain defined threshold dose level. A gradual dose–response may be defined to correlate dose level with 8-OHdG formation in GST-P positive foci and GST-P positive foci induction. Previous mechanistic studies aimed to explain the carcinogenic activity of non-genotoxic carcinogens have shown that the carcinogenic effect only occurs when high doses are used in order to produce prolonged interference with physiological control and modifications of cellular proliferation patterns (Purchase, 1994). Therefore, a perfect threshold of KA may exist for hepatocarcinogenicity in rats.

In conclusion, KA has no initiation activity on rat hepatocarcinogenesis, while high concentrations exert promotion activity, showing the possible existence of a threshold for rat hepatocarcinogenicity.

Conflicts of Interest

The authors declare that there are no conflicts of interest.

Acknowledgements

The authors would like to thank Kang Jin Seok for pathological morphology suggestion and Kaori Touma, Masayo Inoue and Rie Onodera for technical support.

References

Bolt, H.M., Foth, H., Hengstler, J.G., Degen, G.H., 2004. Carcinogenicity categorization of chemicals – new aspects to be considered in a European perspective. Toxicol. Lett. 151, 29–41.

Bray, G.A., Fisher, D.A., Chopra, I.J., 1976. Relation of thyroid hormones to bodyweight. Lancet 307 (7971), 1206–1208.

Burdock, G.A., Soni, M.G., Carabin, I.G., 2001. Evaluation of health aspects of kojic acid in food. Regul. Toxicol. Pharmacol. 33, 80–101.

Fujimoto, N., Watanabe, H., Nakatani, T., Roy, G., Ito, A., 1998. Induction of thyroid tumors in (C57BL/6N X C3H/N)F1 mice by oral administration of kojic acid. Food Chem. Toxicol. 36, 697–703.

Fujimoto, N., Onodera, H., Mitsumori, K., Tamura, T., Maruyama, S., Ito, A., 1999. Changes in thyroid function during development of thyroid hyperplasia induced by kojic acid in F344 rats. Carcinogenesis 20 (8), 1567–1571.

Hengstler, J.G., Bogdanffy, M.S., Bolt, H.M., Oesch, F., 2003. Challenging dogma: thresholds for genotoxic carcinogens? The case of vinyl acetate. Annu. Rev. Pharmacol. Toxicol. 43, 485–520.

Higa, Y., Kawabe, M., Nabae, K., Toda, Y., Kitamoto, S., Hara, T., Tanaka, N., Kariya, K., Takahashi, M., 2007. Kojic acid – absence of tumor-initiating activity in rat liver, and of carcinogenic and photo-genotoxic potential in mouse skin. J. Toxicol. Sci. 32 (2), 143–159.

Ito, N., Tamano, S., Shirai, T., 2003. A medium-term rat liver bioassay for rapid *in vivo* detection of carcinogenic potential of chemicals. Cancer Sci. 94 (1), 3–8.

Ito, N., Tatematsu, M., Hasegawa, R., Tsuda, H., 1989. Medium-term bioassay system for detection of carcinogens and modifiers of hepatocarcinogenesis utilizing the GST-P positive liver cell focus as an endpoint marker. Toxicol. Pathol. 17 (4), 630–641.

Kasai, H., 1997. Analysis of a form of oxidative DNA damage, 8-hydroxy-2′-deoxyguanosine, as a marker of cellular oxidative stress during carcinogenesis. Mutat. Res. 387, 147–163.

Kirsch-Volders, M., Aardema, M., Elhajouji, A., 2000. Concepts of threshold in mutagenesis and carcinogenesis. Mutat. Res. 464, 3–11.

Klaunig, J.E., Kamendulis, L.M., 2004. The role of oxidative stress in carcinogenesis. Annu. Rev. Pharmacol. Toxicol. 44, 239–267.

Mitsumori, K., Onodera, H., Takahashi, M., Funakoshi, T., Tamura, T., Yasuhara, T., Takegawa, K., Takahashi, M., 1999. Promoting effects of kojic acid due to serum TSH elevation resulting from reduced serum thyroid hormone levels on development of thyroid proliferative lesions in rats initiated with N-*bis*(2-hydroxypropyl)nitrosamine. Carcinogenesis 20, 173–176.

Moto, M., Mori, T., Okamura, M., Kashida, Y., Mitsumori, K., 2006. Absence of liver tumor-initiating activity of kojic acid in mice. Arch. Toxicol. 80 (5), 299–304.

Marugame, T., Kamo, K., Katanoda, K., Ajiki, W., Sobue, T., 2006. Cancer incidence and incidence rates in Japan in 2000: Estimates based on data from 11 population-based cancer registries. Jpn. J. Clin. Oncol. 36 (10), 668–675.

Nohynek, J.G., Kirkland, D., Marzin, D., Toutain, H., Leclerc-Ribaud, C., Jinnai, H., 2004. An assessment of genotoxicity and human health risk of tropical use of kojic acid [5-hydroxy-2-(hydroxymethyl)-4H-pyran-4-one]. Food Chem. Toxicol. 42, 93–105.

Purchase, I.F.H., 1994. Current knowledge of mechanisms of carcinogenicity: genotoxins versus non-genotoxins. Hum. Exp. Toxicol. 13, 17–28.

Takada, N., Matsuda, T., Otoshi, T., Yano, Y., Otani, S., Hasegawa, T., Nakae, D., Konishi, Y., Fukushima, S., 1994. Enhancement by organosulfur compounds from garlic and onions of diethylnitrosamine-induced glutathione S-transferase positive foci in the rat liver. Cancer Res. 54 (11), 2895–2899.

Takada, N., Yano, Y., Wanibushi, H., Otani, S., Fukushima, S., 1997. S-methylcysteine and cysteine are inhibitors of induction of glutathione S-transferase placental form-positive foci during initiation and promotion phases of rat hepatocarcinogenesis. Jpn. J. Cancer Res. 88 (5), 435–442.

Takizawa, T., Imai, T., Onose, J., Ueda, M., Tamura, T., Mitsumori, K., Izumi, K., Hirose, M., 2004. Enhancement of hepatocarcinogenesis by kojic acid in rat two-stage models after initiation with N-*bis*(2-hydroxypropyl)nitrosamine or N-diethylnitrosamine. Toxicol. Sci. 81, 43–49.

Takizawa, T., Mitsumori, K., Tamura, T., Nasu, M., Ueda, M., Imai, T., Hirose, M., 2003. Hepatocellular tumor induction in heterozygous *p53*-deficient CBA mice by a 26-week dietary administration of kojic acid. Toxicol. Sci. 73, 287–293.

Tamura, T., Mitsumori, K., Onodera, H., Fujimoto, N., Yasuhara, K., Takegawa, K., Takagi, H., Hirose, M., 2001. Dose-threshold for thyroid tumor-promoting effects of orally administered kojic acid in rats after initiation with *N-bis*(2-hydroxypropyl)nitrosamine. J. Toxicol. Sci. 26 (2), 85–94.

Tsuda, H., Matsumoto, K., Ogino, H., Ito, M., Hirono, I., Nagao, M., Sato, K., Cabral, R., Bartsch, H., 1993. Demonstration of initiation potential of carcinogens by induction of preneoplastic glutathione S-transferase P-form-positive liver cell foci: possible *in vivo* assay system for environmental carcinogens. Jpn. J. Cancer Res. 84 (3), 230–236.

Tsuda, H., Takahashi, S., Yamaguchi, S., Ozaki, K., Ito, N., 1990. Comparison of initiation potential of 2-amino-3-methylimidazo[4,5-f]quinoline and 2-amino-3,8-dimethylimidazo[4,5-f]quinoxaline in an *in vivo* carcinogen bioassay system. Carcinogenesis 11 (4), 549–552.

Umemura, T., Kai, S., Hasegawa, R., Sai, K., Kurokawa, Y., Williams, G.M., 1999. Pentachlorophenol (PCP) produces liver oxidative stress and promotes but does not initiate hepatocarcinogenesis in B6C3F1 mice. Carcinogenesis 20 (6), 1115–1120.

Watanabe, T., Mori, T., Kitamura, Y., Umemura, T., Okamura, M., Kashida, Y., Nishikawa, A., Hirose, M., Mitsumori, K., 2005. Lack of initiating activity of kojic acid on hepatocarcinogenesis in F344 rats. J. Toxicol. Pathol. 18, 79–84.

Wei, C.I., Huang, T.S., Fernando, S.Y., Chung, K.T., 1991. Mutagenicity studies of kojic acid. Toxicol. Lett. 59, 213–220.

Tumor-associated MUC5AC stimulates *in vivo* tumorigenicity of human pancreatic cancer

HIROTAKA HOSHI[1,3], TETSUJI SAWADA[2], MOTOYUKI UCHIDA[1], HIKARU SAITO[1], HIROKO IIJIMA[1], MIKAKO TODA-AGETSUMA[1], TSUTOMU WADA[1], SADAAKI YAMAZOE[2], HIROAKI TANAKA[2], KENJIRO KIMURA[2], ANNA KAKEHASHI[3], MIN WEI[3], KOSEI HIRAKAWA[2] and HIDEKI WANIBUCHI[3]

[1]Biomedical Research Laboratories, Kureha Corporation, 3-26-2 Hyakunin-cho, Shinjuku-ku, Tokyo 169-8503; Departments of [2]Surgical Oncology and [3]Pathology, Osaka City University Graduate School of Medicine, 1-4-3 Asahi-machi, Abeno-ku, Osaka 545-8585, Japan

Received September 30, 2010; Accepted November 8, 2010

DOI: 10.3892/ijo.2011.911

Abstract. MUC5AC, a high molecular weight glycoprotein, is overexpressed in the ductal region of human pancreatic cancer but is not detectable in the normal pancreas, suggesting its association with disease development. In the present study, we investigated the *in vitro* and *in vivo* effects of MUC5AC knockdown by short interfering RNA (siRNA) in the MUC5AC-overexpressing SW1990 and BxPC3 human pancreatic cancer cell lines in order to clarify its function. Significant decreases in the expression levels of MUC5AC mRNA and protein were observed in SW1990 and BxPC3 cells that had been stably transfected with a MUC5AC siRNA expression vector (SW1990/si-MUC5AC and BxPC3/si-MUC5AC cells) compared to those in cells transfected with an si-mock vector (SW1990/si-mock and BxPC3/si-mock cells). In *in vitro* studies, neither type of MUC5AC-knockdown cell showed any difference in cell survival, proliferation, or morphology from the si-mock cells or parental cells. However, *in vivo* xenograft studies demonstrated that MUC5AC knockdown significantly reduced the tumorigenicity and suppressed the tumor growth of si-MUC5AC cells compared to those of the si-mock cells. Immunohistochemical analysis revealed that CD45R/B220$^+$ and Gr-1$^+$ cells had infiltrated into the tumor tissue of the SW1990/si-MUC5AC cells. Furthermore, cancer-associated antigen specific antibodies were detected at high levels in the sera from the SW1990/si-MUC5AC cell-bearing mice. These results suggest that tumor-associated MUC5AC expressed on the surface of pancreatic cancer cells supports the escape of pancreatic cancer cells from immunosurveillance. The present findings highlight a new dimension of MUC5AC as a functional immunosuppressive agent and its important role in pancreatic cancer progression.

Correspondence to: Dr Tetsuji Sawada, Department of Surgical Oncology, Osaka City University Graduate School of Medicine, 1-4-3 Asahi-machi, Abeno-ku, Osaka 545-8585, Japan
E-mail: m1355299@med.osaka-cu.ac.jp

Key words: MUC5AC, mucin, glycoprotein, immunosuppression, short interfering RNA (siRNA), pancreatic cancer

Introduction

Mucins are heavily glycosylated proteins that are expressed in mucosal tissues, establish a selective molecular barrier at the epithelial surface, and engage in signal transduction pathways that regulate morphogenesis. Mucins can be classified into MUC1-20, which each have characteristic tandem repeat sequences. The amino acid residues of mucin are rich in serine and threonine, so have the potential to be O-glycosylated, and sugar chains constitute up to 80% of their molecular weight (1). In addition, mucins influence many cellular processes including growth, differentiation, transformation, adhesion, invasion, and immune surveillance. According to their cellular localization, mucins are divided into two classes: membrane bound mucins and secreted mucins. The secreted mucins, which lack a transmembrane domain and are secreted into extracellular spaces, include MUC2, MUC5AC, MUC5B, MUC6, MUC7, MUC8, and MUC19. The expression of secreted mucins is restricted to secretory organs and cell types. The membrane bound mucins, which are type I membrane proteins, include MUC1, MUC3, MUC4, MUC12, MUC13, MUC15, MUC16, MUC17, and MUC20. The membrane bound mucins are also considered to act as sensors of the external environment. Alterations in the gene expression of mucins accompany the development of cancer and influence cellular growth, differentiation, transformation, adhesion, and invasion (2-14). For example, aberrant expression of MUC4 in pancreatic, lung, breast, colon, and ovarian malignancies potentiates tumor cell growth and metastasis by altering the behavioral properties of tumor cells (15). MUC2-deficient mice showed increased proliferation, decreased apoptosis, and increased intestinal epithelial cell infiltration and frequently developed small intestinal, rectal, and gastrointestinal tumors (16). These results showed that MUC2 is involved in the suppression of cancer that protect the gastrointestinal tract.

It has been reported that MUC5AC is aberrantly expressed in premalignant and malignant lesions as well as in several pancreatic cancer cell lines, but is undetectable in normal pancreatic tissue (17-21; Ho *et al*, Gastroenterology 118: abs. 664, 2000). In our previous study, MUC5AC was expressed in 89.6% (60 of 67 cases) of pancreatic cancer cases (unpublished data). However, the details of how MUC5AC is involved in the process of malignant transformation, proliferation, and metastasis in pancreatic cancer remain to be elucidated. In the present study, we adapted the small interfering RNA (siRNA) technique to suppress MUC5AC expression in human pancreatic cancer cells and evaluated the effect of MUC5AC-knockdown on human pancreatic cancer cells *in vitro* and *in vivo* to clarify its functional role in human pancreatic cancer progression.

Materials and methods

Materials. The human pancreatic cancer cell lines SW1990, BxPC3, and PK-45P were purchased from Summit Pharmaceuticals International Corp. (Tokyo, Japan), Dainippon Sumitomo Pharma Biomedical Co. Ltd. (Osaka, Japan), and Cell Resource Center for Biomedical Research, Institute of Development, Aging and Cancer Tohoku University (Miyagi, Japan), respectively. The mouse anti-human MUC5AC monoclonal antibody (K-MAC5, IgG1) was developed in our laboratory. The rat anti-mouse CD45R/B220 monoclonal antibody (clone RA3-6B2) against B lymphocytes and the Ly-6G and Ly-6C (Gr-1, clone RB6-8C5) monoclonal antibody against granulocytes were purchased from Becton-Dickinson (San Jose, CA).

Mice. The experimental protocol was approved by the Ethics Committee on Animal Experiments of the Biomedical Research Laboratories of Kureha Corp., and the mice were treated in accordance with the guidelines of the committee. Five-week-old specific-pathogen-free female BALB/c-nu/nu mice purchased from Charles River Japan, Inc. (Kanagawa, Japan) were acclimatized for one week and then used in the experiments at the age of six weeks. The mice were allowed free access to sterilized CE-2 food (Oriental Yeast, Tokyo, Japan) and sterilized tap water and were bred at 25±2˚C, a humidity of 55±7%, laminar flow, and under a 12-h light/12-h dark cycle at 150-300 lux. To maintain a uniform environment, noise was carefully avoided, and only the experimenters and keepers were allowed into the animal room.

Cell culture conditions. SW1990 cells were cultured in Dulbecco's modified Eagle's medium (DMEM; Invitrogen Corp., San Diego, CA) supplemented with 10% fetal bovine serum (FBS; Biowest, Nuaill, France), 50 IU/ml penicillin, and 50 μg/ml streptomycin. BxPC3 and PK-45P cells were cultured in Roswell Park Memorial Institute (RPMI)-1640 (Invitrogen) supplemented with 10% FBS (Biowest), 50 IU/ml penicillin, and 50 μg/ml streptomycin. The cells were grown at 37˚C under 5% CO_2 in a humidified atmosphere and passaged before they reached confluency using 0.25% (w/v) trypsin solution containing 0.04% (w/v) EDTA.

Construction of the siRNA expression vector. Eight types of siRNA sequences (19-mer) against human MUC5AC were designed using a computer algorithm and tested for silencing efficacy in transient assays. The MUC5AC siRNA target sequence 5'-TTTGAGAGACGAAGGATAC-3' was found to be the sequence showing the most marked effects and cloned in order to generate a stable siRNA expressing construct into the p*Silencer* 3.1-H1 neo vector (Ambion, Inc., Austin, TX). Briefly, oligonucleotides (64-mer) encoding 19-mer hairpin sequences specific to the mRNA target were designed. These contained two complementary domains (sense and antisense) separated by the loop sequence 5'-TTCAAGAGA-3'. Double-stranded oligonucleotides were ligated into the p*Silencer* 3.1-H1 neo vector at *Bam*HI (Takara Bio Inc., Shiga, Japan) and *Hin*dIII (TaKaRa) restriction sites (p*Silencer*/si-MUC5AC). The plasmid was then amplified in chemically competent *Escherichia coli* (DH5α cells).

Quantitative real-time PCR. Quantitative real-time PCR (qRT-PCR) was performed with a Light Cycler system (Roche Diagnostics K.K., Tokyo, Japan) using the Light Cycler DNA master SYBR-Green I kit (Roche Diagnostics K.K.) according to the manufacturer's protocol. The following primers were used: for human MUC5AC gene: 5'-GCCACCGCTGCGGC CTTCTTC-3' (forward) and 5'-GTGCACGTAGGAGGACA GCGC-3' (reverse) and for human *glyceraldehyde-3-phosphate dehydrogenase (GAPDH)* gene: 5'-GAAGGTGAAGGTCGG AGTC-3' (forward) and 5'-GAAGATGGTGATGGGAT TTC-3' (reverse). *GAPDH* gene expression was used for cDNA normalization. Amplification was carried out as follows: initial denaturation at 95˚C for 15 min, followed by 40 cycles at 95˚C for 10 sec, a touchdown annealing (0.5˚C/cycle) from 68-60˚C for 10 sec, and elongation at 72˚C for 10 sec. After the completion of PCR amplification, a melting curve analysis was performed.

Transfection and selection of clones. SW1990 and BxPC3 cells were transfected with pSilencer/si-MUC5AC as a target vector or p*Silencer*/si-mock as a control vector using Genejuice (Merck, Darmstadt, Germany) according to the manufacturer's instructions. Briefly, the cells were seeded in a 100-mm culture dish and grown to 60-80% confluence. The medium was then removed, and the cells were washed twice in serum-free medium, before being incubated for 8 h in 15 ml serum-free medium with 18 μl Genejuice and 6 μg plasmid DNA. The cells were then washed in medium and cultured for 24 h in complete medium, and each cell was subcultured after 48 h (~5-fold). SW1990 and BxPC3 cells were selected by culturing them in the presence of geneticin at 600 and 400 μg/ml, respectively. The efficiency of MUC5AC-knockdown was tested by qRT-PCR and FACS analysis.

Fluorescence-activated cell sorting (FACS) analysis. The cells were detached using 0.04% (w/v) EDTA, washed with PBS, and resuspended in PBS containing 2% FBS and 2 mM EDTA (FACS buffer) and then were incubated with an appropriate dilution of K-MAC5 (1 μg), mouse serum (100-fold dilution), or isotype control (1 μg) per 10^6 cells for 2 h at 4˚C. After being washed three times in FACS buffer, the cells were incubated with a FITC-conjugated rabbit anti-mouse secondary antibody (Becton-Dickinson) for 30 min at 4˚C. The cells were then washed three times and resuspended

in FACS buffer, before being analyzed on a FACScan (Becton-Dickinson) with $>10^4$ cells analyzed per sample. The data files were analyzed using CellQuest (Becton-Dickinson), and the cells were gated using forward and side scatter variables to eliminate dead cells and debris.

Cell proliferation assay. The cells were suspended in each medium at a density of $1x10^4$/ml, and 100 μl suspensions were seeded in 96-well plates. After incubation for 0, 1, 2, 3, or 4 days, 20 μl of 3-(4,5-dimethylthiazol-2-yl)-2,5-diphenyltetrazolium bromide (MTT) solution (5 mg/ml) was added. Following incubation at 37°C for 3 h, the supernatant was removed, and dimethylsulfoxide (DMSO) was added at 100 μl/well. The absorbance of formazan was measured at a wavelength of 570 nm and a reference wavelength of 630 nm with a Bio-Rad Microplate Reader 550 (Bio-Rad Laboratories Inc. Tokyo, Japan). Cell growth curves were plotted from the mean ± standard deviation (SD).

Tumorigenicity assay in xenograft models. Exponentially growing cells were detached with 0.25% (w/v) trypsin solution containing 0.04% (w/v) EDTA and resuspended in PBS at a density of $1x10^8$/ml. Each cell line ($1x10^7$/mice) was implanted s.c. into the flanks of nude mice, and their body weight and tumor volume were measured at least once a week. To determine tumor volume, two bisecting diameters were measured using a slide caliper, and the tumor volumes were calculated using the following formula: tumor volume = length x $(\text{width})^2$ x 0.5236 (22). At the end of the experiment, the tumors were removed, weighed, and fixed in 10% formaldehyde neutral buffer solution. Ten mice were used for each cell line. Tumors growth curves were plotted as the mean volume ± standard error (SE).

Metastasis assay. The experimental lung colonization was evaluated by injecting $1x10^6$ viable cells in 100 μl of PBS i.v. into the lateral tail vein of the BALB/c-nu/nu mice. The mice were euthanized on day 30 posttransplantation, their lungs were removed, and the total number of surface colonies was estimated under a dissecting microscope. Ten mice were used for each cell line.

Histology and immunohistochemistry. Lymphocyte infiltration into tumor tissue was evaluated by immunohistochemical analysis. Tumor tissues fixed in 10% formaldehyde neutral buffer solution were embedded in paraffin. Paraffin-embedded sections of 4 μm thickness were deparaffinized with xylene and ethanol, treated with 3% hydrogen peroxide solution for 20 min to inactivate endogenous peroxidase, and blocked with 2% porcine plasma in TBS for 15 min to reduce non-specific binding. Then, K-MAC5 monoclonal antibody, rat anti-mouse CD45R/B220 and Gr-1 monoclonal antibodies were added, and the sections were incubated at room temperature for 1 h. After being washed three times with TBS containing 0.05% Tween-20 (TBS-T), a horseradish peroxidase-labeled secondary antibody was added, and the sections were incubated at room temperature for 30 min. After being washed a further three times with TBS-T, immunoreaction was visualized with Liquid DAB Chromogen (Dako Japan Co. Ltd., Kyoto, Japan), and the sections were counterstained with hematoxylin. After being mounted on a glass slide with Entellan Neu (Merck), the stained specimens were examined using a microscope. In parallel to the immunostaining, hematoxylin and eosin (H&E) staining was performed for morphological evaluation.

Secondary tumor challenge. The primary tumor (SW1990/si-MUC5AC cells) was implanted via the injection of $1x10^7$ cells into the right flanks of nude mice. After 42 days, a secondary tumor (SW1990/si-mock cells) was implanted on the opposite flank. Tumor growth was measured at least once a week according to the above method.

Statistical analysis. All data are expressed as means ± SD or SE. Statistical significance was determined by the Student's t-test. P-values <0.05 were considered significant.

Results

Establishment of MUC5AC-knockdown cells by siRNA. The MUC5AC-overexpressed human pancreatic cancer cell lines SW1990 and BxPC3 were transfected with the p*Silencer* 3.1-H1 neo/si-MUC5AC vector or the p*Silencer* 3.1-H1 neo/si-mock vector as a negative control, and stable transfectants were established. In order to confirm the silencing efficiency of MUC5AC siRNA, the MUC5AC mRNA and protein levels in the transfectants were determined by qRT-PCR and FACS analysis. qRT-PCR data showed that MUC5AC expression was significantly decreased in stably transfected cells containing MUC5AC siRNA (SW1990/si-MUC5AC and BxPC3/si-MUC5AC cells) compared with si-mock cells containing the control vector (SW1990/si-mock and BxPC3/si-mock cells) (Fig. 1A). The loss of MUC5AC from the cell surface was determined by FACS analysis. It was found that the surface expression of MUC5AC was also substantially down-regulated in SW1990/si-MUC5AC and BxPC3/si-MUC5AC cells (si-MUC5AC transfectants) compared with the SW1990/si-mock and BxPC3/si-mock cells (si-mock transfectants), respectively (Fig. 1B). However, there were no differences between the si-mock transfectants and parental cells with regard to their mRNA and protein expression levels (data not shown). Therefore, in the following experiments, SW1990/si-mock and BxPC3/si-mock cells were used as negative controls.

In vitro cell survival, proliferation, and morphology. To investigate the effect of MUC5AC on cell proliferation, SW1990/si-mock, SW1990/si-MUC5AC, BxPC3/si-mock, and BxPC3/si-MUC5AC cells were seeded in 96-well plates and the number of cells was determined over time. As shown in Fig. 2A and B, no difference in cell proliferation was observed between the SW1990/si-MUC5AC and SW1990/si-mock cells or between the BxPC3/si-MUC5AC and BxPC3/si-mock cells. Next, we examined whether the knockdown of MUC5AC was associated with any morphological changes. Each cell was plated, and morphological changes were assessed during proliferation from sparsity to confluence. As a result, the SW1990/si-MUC5AC and BxPC3/si-MUC5AC cells tended to cluster together, and some of them exhibited a fibroblast-like morphology and a tightly packed cobblestone-like morphology, respectively (Fig. 2C), but the difference in

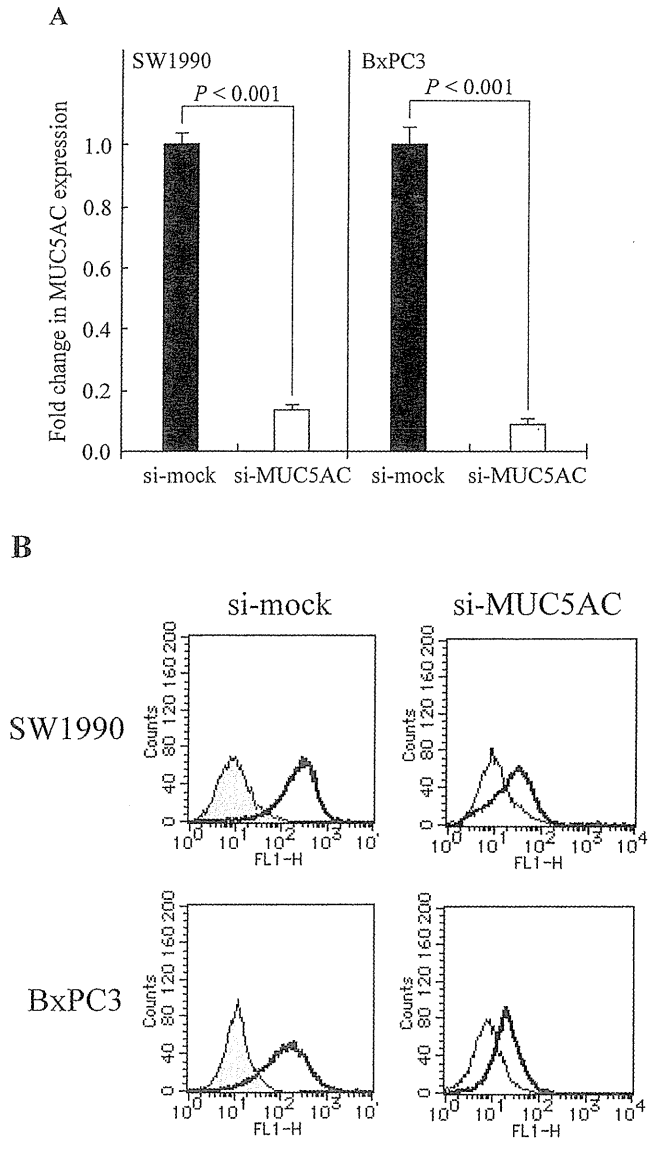

Figure 1. Establishment of MUC5AC-knockdown human pancreatic cancer cell lines. SW1990 and BxPC3 cells were stably transfected with p*Silencer* 3.1-H1 neo/si-mock or p*Silencer* 3.1-H1 neo/si-MUC5AC (an MUC5AC specific siRNA expression vector). The MUC5AC expression of each cell was then analyzed by qRT-PCR and FACS as described in Materials and methods. (A) MUC5AC and GAPDH mRNA expression levels were evaluated by qRT-PCR. qRT-PCR was performed on cDNA from each cultured cells using human MUC5AC-specific primers. Values were normalized using the internal control gene, *GAPDH*. All PCR experiments were performed in triplicate. Columns, mean of triplicate determinations; bars, SD. (B) FACS analysis of MUC5AC expression in mock- and MUC5AC-knockdown cells. Fluorescence of MUC5AC expressing SW1990 and BxPC3 cells probed with K-MAC5 mAb. Top, SW1990/si-mock and SW1990/si-MUC5AC cells; bottom, BxPC3/si-mock and BxPC3/si-MUC5AC cells; gray filled histograms, isotypic control antibody; bold lines, K-MAC5. The experiment was repeated twice. Representative data are shown.

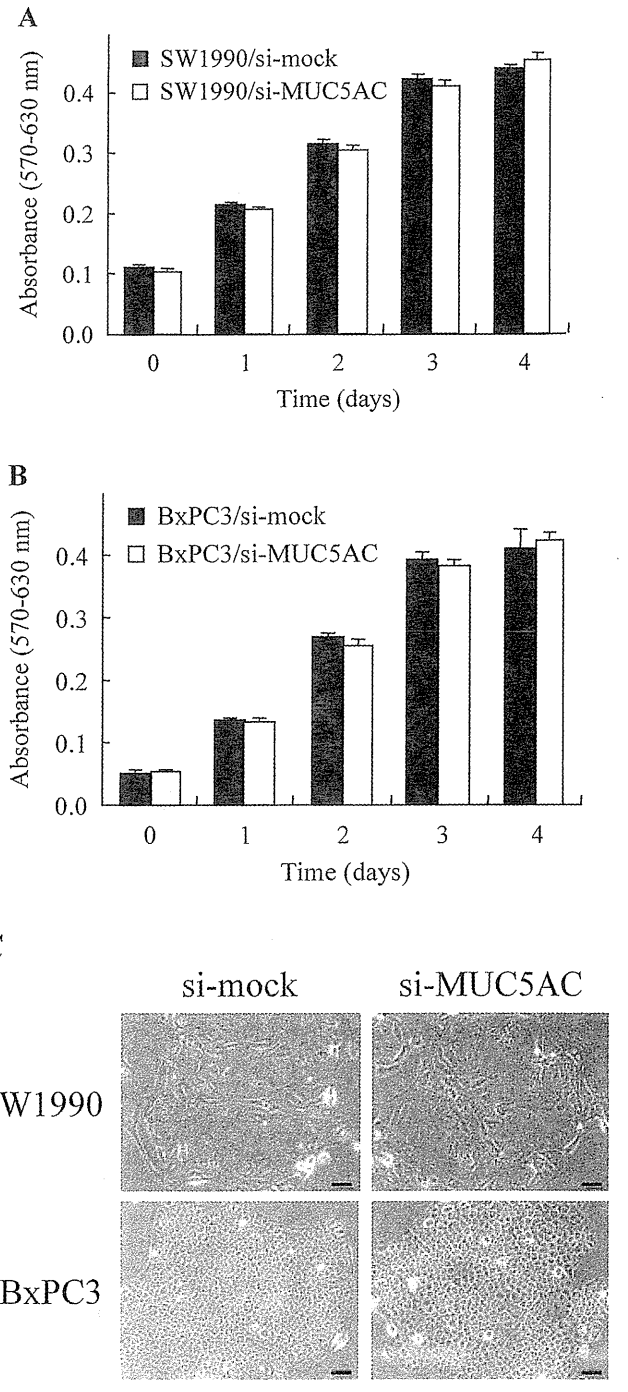

Figure 2. Effect of MUC5AC on cell growth and morphologic change. SW1990/si-mock and SW1990/si-MUC5AC (A) or BxPC3/si-mock and BxPC3/si-MUC5AC cells (B) seeded in a 96-well plate were cultured for 0, 1, 2, 3, or 4 days. Filled columns, si-mock cells; open columns, si-MUC5AC cells. Their cell number was determined by their absorbance as described in Materials and methods. The experiment was repeated thrice. Representative data are shown. Columns, mean of triplicate determinations; bars, SD. SW1990/si-mock and SW1990/si-MUC5AC (C, top) or BxPC3/si-mock and BxPC3/si-MUC5AC cells (C, bottom) were cultured during proliferation from sparsity to confluence, and phase-contrast microscopic images were observed. The experiment was repeated thrice. Data shown are representative images captured from one of three independent experiments performed in triplicate. Bar, 50 μm.

morphology between the si-mock and si-MUC5AC cells was not marked.

In vivo tumorigenicity and metastatic potential. As both the si-mock and si-MUC5AC cells showed exactly the same proliferation rate *in vitro*, we examined their ability to induce tumorigenicity *in vivo*. SW1990/si-MUC5AC cell-challenged mice barely developed any visible solid tumors, but the si-mock cell-challenged mice had developed tumors by one week as expected (Fig. 3A). The tumor growth of the SW1990/si-MUC5AC cells was suppressed compared to that of the

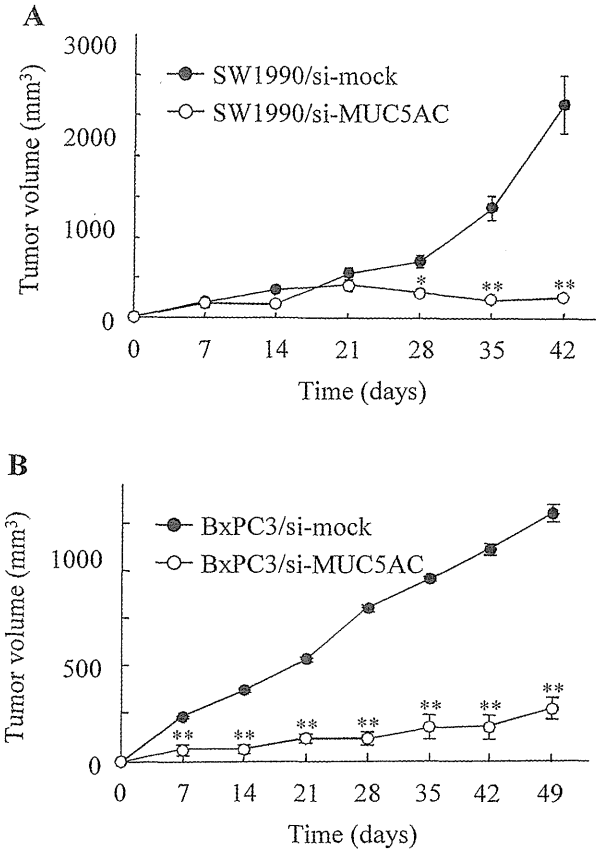

Figure 3. MUC5AC-knockdown by siRNA significantly inhibited tumor xenograft growth. (A) Tumor growth curves of SW1990/si-mock (filled circles) and SW1990/si-MUC5AC (open circles) cells. (B) Tumor growth curves of BxPC3/si-mock (filled circles) and BxPC3/si-MUC5AC (open circles) cells. The cells were s.c. implanted with $1x10^7$ cells into the nude mice on day 0. The mice were monitored for tumor formation until 42 (A) and 49 (B) days, respectively, and the tumors were measured on the indicated days. These experiments were repeated at least thrice. Representative data are shown. Points, mean tumor volume of 10 mice for each group; bars, SE. Statistically significant at $^*P<0.005$ and $^{**}P<0.001$ (versus si-mock cell-challenged mice group).

SW1990/si-mock cells after day 28 ($P<0.005$). Also tumor volumes were significantly increased in the mice injected with BxPC3/si-mock cells compared with the tumor growth in those injected with BxPC3/si-MUC5AC cells (Fig. 3B). The tumor growth of the BxPC3/si-MUC5AC cells was decreased compared with that of the BxPC3/si-mock cells after day 7 ($P<0.001$). Furthermore, to examine whether the proliferation of si-MUC5AC cells was also inhibited in a lung metastasis model, the SW1990/si-mock and SW1990/si-MUC5AC cells were injected i.v. into nude mice, and metastases were enumerated after day 30. As a result, there were no lung metastases that could be confirmed under a dissecting microscope in the SW1990/si-MUC5AC cell-challenged mice, while many metastases were observed in the SW1990/si-mock cell-challenged mice (Table I).

Accumulation of immunocytes in the tumor tissues. To identify the types of immunocytes that infiltrated into the tumor tissues, the tumor challenge sites were removed and subjected to histological and immunohistochemical examination. First, MUC5AC expression at the SW1990/si-mock cell-challenged site and SW1990/si-MUC5AC cell-challenged site was examined by IHC using K-MAC5 monoclonal antibody, and its significant suppression at the latter site was confirmed (Fig. 4A). Next, rat anti-mouse CD45R/B220 and Gr-1 monoclonal antibodies were used for the detection of the B lymphocytes and granulocytes, respectively. As shown in Fig. 4B, H&E staining showed that many immunocytes had infiltrated into the SW1990/si-MUC5AC cell-challenged site. Immunohistochemistry revealed that the infiltrating cells were CD45R/B220$^+$ (Fig. 4C) and Gr-1$^+$ cells (Fig. 4D) that were scattered throughout the tumor, but were particularly localized in the epithelial and surrounding stromal compartments. In contrast, few or no infiltrating immunocytes were found at the SW1990/si-mock cell-challenged site.

Table I. MUC5AC-knockdown in tumor cells significantly diminishes lung metastasis.[a]

	Count of lung metastases									
Mice no.	1	2	3	4	5	6	7	8	9	10
SW1990/ si-mock	4	10	3	5	6	8	7	6	10	4
SW1990/ si-MUC5AC	0	0	0	0	0	0	0	0	0	0

[a]Tumor cells ($1x10^6$) were injected into the lateral tail veins of the mice. The lungs were collected 30 days after posttransplantation, and the total numbers of surface colonies were counted. Ten mice were used for each cell line. The experiment was repeated twice. Representative data are shown.

Antibody production by B lymphocytes. As it was shown in the above immunostaining examination that many B lymphocytes had accumulated at the SW1990/si-MUC5AC cell-challenged site, we investigated whether B lymphocytes raised specific antibodies against the implanted tumor cells. To do this, sera were collected from SW1990/si-mock and SW1990/si-MUC5AC cell-challenged mice and were used to evaluate the responsiveness to human pancreatic PK-45P cells, which do not express MUC5AC, by FACS analysis. FACS analysis showed that the sera of the SW1990/si-MUC5AC cell-challenged mice more effectively recognized PK-45P cells as a foreign substance, compared to that of the SW1990/si-mock cell-challenged mice (Fig. 4E).

Rejection of a secondary challenge with SW1990/si-mock cells in mice subjected to primary challenge with SW1990/si-MUC5AC cells. It was thought that memory B cells may play a pivotal role in the rejection of grafted SW1990/si-MUC5AC cells in nude mice. So, we investigated whether a secondary challenge with SW1990/si-mock cells would be rejected in mice that had previously been challenged with SW1990/si-MUC5AC cells. As a first step, SW1990/si-MUC5AC cells (the primary tumor) were implanted into the right flanks of nude mice. After 42 days, SW1990/si-mock cells

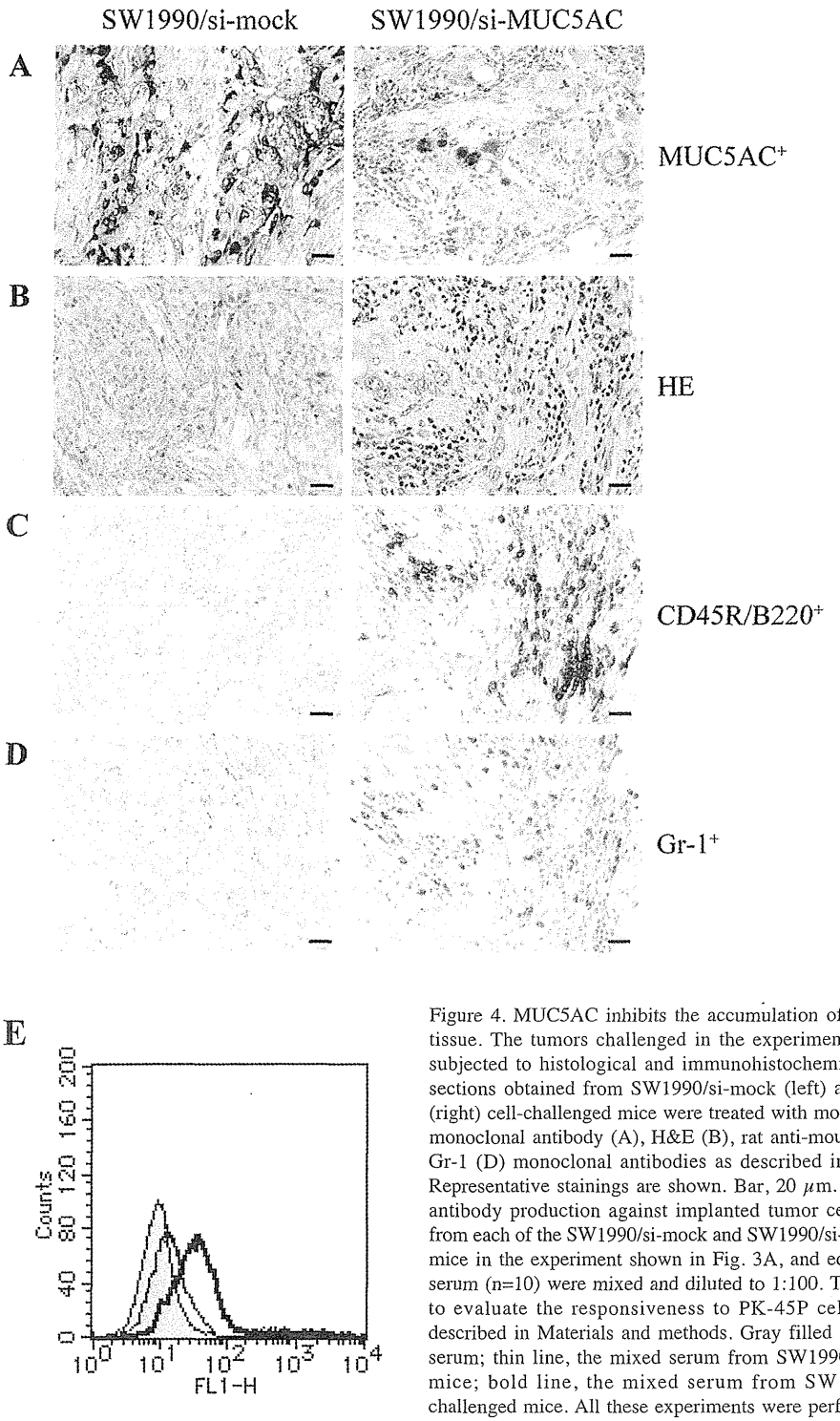

Figure 4. MUC5AC inhibits the accumulation of immunocytes into tumor tissue. The tumors challenged in the experiment shown in Fig. 3A were subjected to histological and immunohistochemical examinations. Tumor sections obtained from SW1990/si-mock (left) and SW1990/si-MUC5AC (right) cell-challenged mice were treated with mouse anti-human MUC5AC monoclonal antibody (A), H&E (B), rat anti-mouse CD45R/B220 (C), and Gr-1 (D) monoclonal antibodies as described in Materials and methods. Representative stainings are shown. Bar, 20 μm. (E) MUC5AC suppresses antibody production against implanted tumor cells. Serum was collected from each of the SW1990/si-mock and SW1990/si-MUC5AC cell-challenged mice in the experiment shown in Fig. 3A, and equivalent amounts of each serum (n=10) were mixed and diluted to 1:100. The mixed serum was used to evaluate the responsiveness to PK-45P cells by FACS analysis as described in Materials and methods. Gray filled histogram, normal control serum; thin line, the mixed serum from SW1990/si-mock cell-challenged mice; bold line, the mixed serum from SW1990/si-MUC5AC cell-challenged mice. All these experiments were performed at least thrice. One representative data set of three independent experiments is shown.

(the secondary tumor) were implanted into the opposite flank (Fig. 5A). As a result, the secondary tumor growth of SW1990/si-mock cells was significantly decreased in the primary tumor-bearing mice compared with the primary tumor-absent mice (Fig. 5B). Significant inhibition was shown after day 7 of the secondary challenge ($P<0.001$). In other words, the primary graft of SW1990/si-MUC5AC cells caused strong rejection of the secondary tumor graft. Furthermore, the primary tumor no longer developed and was not promoted by the secondary inoculation (data not shown). In contrast, the tumor volumes of the SW1990/si-mock cells in the primary tumor-absent mice were significantly increased, as expected from the results shown in Fig. 3A.

Discussion

In spite of recent developments that have improved the prevention, screening, and therapy for pancreatic cancer, it still has a poor prognosis: a 5-year survival rate of up to 3% and a median survival of up to 6-month. This poor prognosis

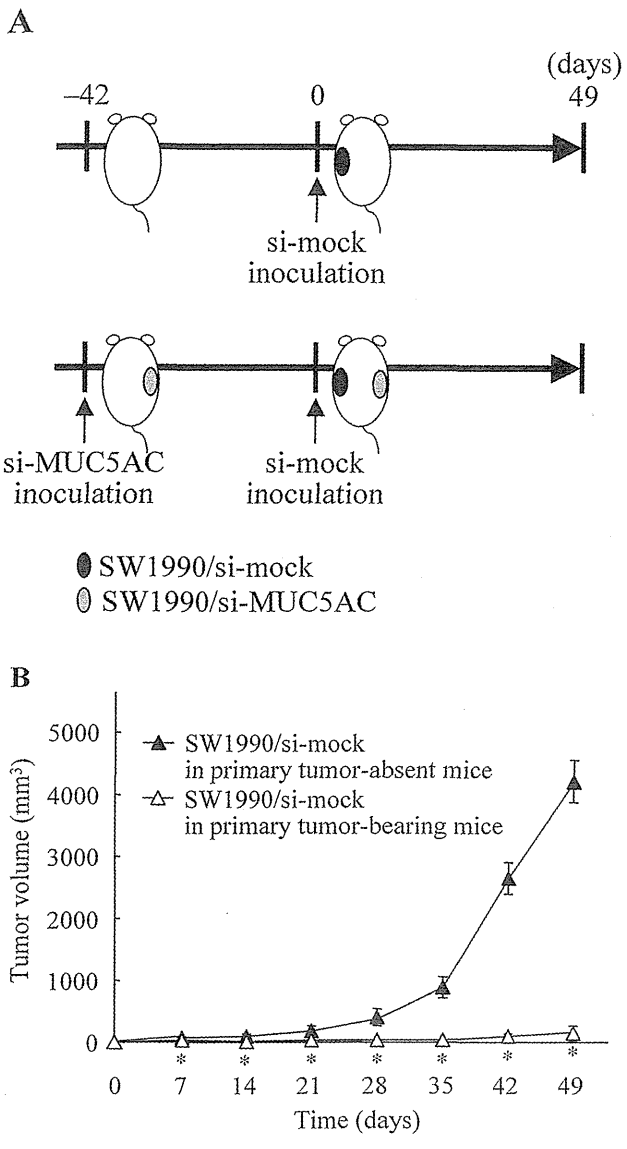

Figure 5. MUC5AC suppresses the immune memory system. (A) Animal experiment protocol. (B) Tumor volume. The primary tumor (SW1990/si-MUC5AC cells) was implanted with $1x10^7$ cells into the flanks of nude mice. After 42 days, a secondary tumor (SW1990/si-mock cells) was implanted with $1x10^7$ cells into the primary tumor-absent mice (filled triangles) and the primary tumor-bearing mice (open triangles). Tumor size was measured on the indicated days. These experiments were repeated at least thrice. Representative data are shown. Points, mean tumor volume of 10 mice for each group; bars, SE. Statistically significant at $^*P<0.001$ (versus primary tumor-absent mice group).

is a consequence of metastatic disease, which results from a lack of early detection and effective treatment. Concerning the relationship between the malignancy grade of pancreatic cancer and mucins, it was previously reported that MUC1 and carbohydrate antigens such as sialyl Lewis antigen are related to metastatic potential and prognosis. For example, Tsutsumida *et al* previously reported that down-regulation of MUC1 expression by siRNA significantly decreased human pancreatic cancer cell proliferation *in vitro* and *in vivo* (23). Chaturvedi *et al* demonstrated that silencing MUC4 expression by transfecting MUC4-specific short hairpin RNA into a human pancreatic cell line decreased cell growth and metastasis *in vivo* and induced ectopic expression of growth- and metastasis-associated genes. They also showed that over-expression of MUC4 is associated with increased tumor cell growth and metastasis via interference with the interaction between cancer cells and extracellular matrix proteins (24).

MUC5AC has been shown to be a major component of the stomach and airway, and little or no expression of MUC5AC is found in other normal tissues; whereas, it is anomalously expressed in human pancreatic and colorectal cancers. This implies that MUC5AC plays an important role in these cancers, but few reports exist on its function. Here, we established MUC5AC-knockdown cells by introducing siRNA and investigated how MUC5AC contributes to tumor progression. The findings from the present study showed that the ectopic expression of MUC5AC was not involved in cell growth *in vitro*, but that it was intimately involved in tumor growth *in vivo*. The expression levels of cell-adhesion factors, some of which, such as sialyl-Lewis^a, sialyl-Lewis^x, and E-cadherin are known to be related to metastasis, were not affected in si-MUC5AC cells (data not shown). In addition, to test the alteration in migratory capacity after the suppression of MUC5AC, we performed a scratch wound-healing assay in si-MUC5AC and si-mock cells. The scratch wound-healing assay is considered to be an *in vitro* model of the epithelial cell migration that occurs during wound healing. The scratch wounds in both cells were closed with a large portion after 48 h and no significant delay in the migration of si-MUC5AC cells into the empty space was observed (data not shown). Therefore, it appears that the functions of MUC5AC in pancreatic cancer are essentially different from those of other mucins. In the future, we are going to perform a microarray analysis of si-mock and si-MUC5AC cells and to investigate the expression of tumor-associated genes.

An analysis of the functional role of MUC5AC was reported for colorectal cancer. It may be assumed that the expression of MUC5A plays a role in the invasiveness of cancers, as it is detected in the early stages of human colorectal cancer. Truant *et al* reported on the invasive properties of the human colon carcinoma cell line HT-29 (HT-29 STD) and its highly MUC5AC secreting-variant (HT-29 5M21). It was found that HT-29 STD cells are non-invasive; whereas, HT-29 5M21 cells are invasive due to a lack of cell-cell adhesion through E-cadherin, and HT-29 STD cells and HT-29 5M21 cells also have different morphologies, the former grows in multilayers, but the latter grows in monolayers (25). In the present study, MUC5AC-knockdown cells and their parental cells proliferated in multilayers and did not differ in morphology (Fig. 2). These results indicate that the MUC5AC molecules of pancreatic and colorectal cancers may have different functions.

In a previous report, mucins were found to have inhibitory effects on the antitumor response of the host and to promote tumor progression and metastasis. Cell-cell adhesion contributes to the normal development and function of cells; whereas, the highly glycosylated rigid structure of the mucins reduces both homotypic cell-cell adhesion and cell-substratum interactions (26). Almost all of the functions of mucins reported until now have been connected to proliferation, adhesion, migration, or invasion, and *in vitro* as well as *in vivo* proliferation has been reported to be inhibited by knockdown

of the expression of mucins. However, the present study demonstrated that MUC5AC-knockdown affected *in vivo* proliferation but not *in vitro* proliferation, which differs from the results of previous reports. As shown in Figs. 2 and 3, MUC5AC-knockdown cells showed similar results to the control cells with regard to cell survival, proliferation, and morphology *in vitro*. However, in *in vivo* xenograft studies, their tumor growth was significantly inhibited compared with that of the control cells. So, why were *in vivo* tumorigenicity and metastasis inhibited when no marked *in vitro* effect was observed? One of the reasons for this inhibitory effect is thought to be induced by antibody-dependent cell-mediated cytotoxicity (ADCC). In the present study, B cells and neutrophils were found to accumulate at SW1990/si-MUC5AC cell-challenged sites (Fig. 4). Moreover, a greater number of antibodies against human pancreatic cells were present in the blood of the SW1990/si-MUC5AC cell-challenged mice compared to the levels produced by the SW1990/si-mock cell-challenged mice (Fig. 4E). Neutrophils are non-specific cytotoxic immunocytes that exclude infecting organisms. Recently, it has been reported that neutrophils also have antitumor effects mediated through ADCC via phagocytosis, elastase, or superoxide (27-29). ADCC is triggered by tumor-specific antibodies and Fc receptor-expressing cytolytic cells such as NK cells, neutrophils, eosinophils, and monocytes/macrophages (30). According to these results, the present *in vivo* tumor inhibition was supposed to be induced by ADCC. Moreover, si-MUC5AC cells are a MUC5AC-knockdown cell line and are not able to grow *in vivo*. The SW1990/si-MUC5AC cell-challenged mice used in this study significantly rejected a secondary tumor challenge with SW1990/si-mock cells, which are usually able to grow *in vivo* (Fig. 5B). As nude mice were used in the present experiments, antigen memory via cytotoxic T cells can not be involved. Therefore, the mice that received the si-MUC5AC cells might have produced specific antibodies against an unknown pancreatic cancer specific antigen, and these antibodies may have inhibited the secondary-challenged si-mock tumor via ADCC. It would be interesting to know which molecule serves as the antigen in this case, as its identification and analysis would provide a target for molecular pancreatic cancer therapeutics.

Another possible reason for the *in vivo* inhibition of tumorigenicity is that MUC5AC is directly involved in immune suppression and avoidance. Several reports have investigated MUC1 or MUC2. Overexpression of MUC1 in pancreatic cancer is associated with poor prognosis (31), and there is disputed evidence that tumors associated with MUC1 directly influence the response of immunocytes. For example, MUC1 inhibits the function of effector cells such as natural killer cells, lymphokine-activated killer cells, and cytotoxic T-cells. Also, soluble MUC1 induces apoptosis of activated T cells and inhibits the proliferation of natural killer cells and cytotoxic T-cells (32,33). MUC2 has been reported to bind to a scavenger receptor of monocytes/macrophages and leads to the overproduction of PGE2, which suppresses immunocytes through COX2 (34,35). In this study, the growth of MUC5AC-knockdown cells was inhibited in not only xenografted tumors but also a lung metastasis mode (Table I). Thus, it has been suggested that MUC5AC may be involved in immunosuppression and evasion from the immune system similarly to MUC1 and MUC2. However, future studies are needed to investigate the immunosuppressive mechanism of MUC5AC in human pancreatic cancer.

In conclusion, we investigated the role of MUC5AC in human pancreatic cancer progression using specific siRNA against MUC5AC. Our data showed that suppression of MUC5AC in two human pancreatic cancer cell lines dramatically reduced *in vivo* tumor growth and metastasis without affecting cell growth *in vitro*. Also infiltration of $CD45R/B220^+$ and $Gr\text{-}1^+$ cells was observed in tumor tissue generated by implanting si-MUC5AC cells into mice. Furthermore, specific antibodies against the tumor cells were mostly observed in the sera of SW1990/si-MUC5AC cell-bearing mice. These results suggested that the MUC5AC expressed on the surface of pancreatic cancer cells aids cancer cell escape from the immune system. The present findings highlight a new dimension of MUC5AC as a functional immunosuppressive agent and its important role in pancreatic cancer progression. Also, MUC5AC may be an important indicator for the diagnosis and prognosis of pancreatic cancer, and disruption of MUC5AC may have potential as a treatment for MUC5AC-expressing pancreatic and other cancers.

Acknowledgements

This work was conducted at Kureha Corporation, Tokyo, Japan and Osaka City University, Osaka, Japan. Hirotaka Hoshi, Motoyuki Uchida, Hikaru Saito, Hiroko Iijima, Mikako Toda-Agetsuma, and Tsutomu Wada are employees of Kureha Corporation, but the study was conducted with scientific integrity and presents no conflict of interest.

References

1. Carlstedt I, Sheehan JK, Corfield AP and Gallagher JT: Mucus glycoproteins: a gel of a problem. Essays Biochem 20: 40-76, 1985.
2. Bobek LA, Tsai H, Biesbrock AR and Levine MJ: Molecular cloning, sequence, and specificity of expression of the gene encoding the low molecular weight human salivary mucin (MUC7). J Biol Chem 268: 20563-20569, 1993.
3. Gum JR Jr, Hicks JW, Swallow DM, *et al*: Molecular cloning of cDNA derived from a novel human intestinal mucin gene. Biochem Biophys Res Commun 171: 407-415, 1990.
4. Gum JR Jr, Hicks JW, Toribara NW, Rothe EM, Lagace RE and Kim YS: The human MUC2 intestinal mucin has cysteine-rich subdomains located both upstream and downstream of its central repetitive region. J Biol Chem 267: 21375-21383, 1992.
5. Gum JR Jr, Hicks JW, Toribara NW, Siddiki B and Kim YS: Molecular cloning of human intestinal mucin (MUC2) cDNA. Identification of the amino terminus and overall sequence similarity to prepro-von Willebrand factor. J Biol Chem 269: 2440-2446, 1994.
6. Gum JR Jr, Crawley SC, Hicks JW, Szymkowski DE and Kim YS: MUC17, a novel membrane-tethered mucin. Biochem Biophys Res Commun 291: 446-475, 2002.
7. Hollingsworth MA and Swanson BJ: Mucins in cancer: protection and control of the cell surface. Nat Rev Cancer 4: 45-60, 2004.
8. Moniaux N, Nollet S, Porchet N, Degand P, Laine A and Aubert JP: Complete sequence of the human mucin MUC4: a putative cell membrane-associated mucin. Biochem J 338: 325-333, 1999.
9. Fauquette V, Aubert S, Groux-Degroote S, Hemon B, Porchet N, van Seuningen I and Pigny P: Transcription factor AP-2 represses both the mucin MUC4 expression and pancreatic cancer cell proliferation. Carcinogenesis 28: 2305-2312, 2007.

10. Porchet N, Pigny P, Buisine MP, Debailleul V, Degand P, Laine A and Aubert JP: Human mucin genes: genomic organization and expression of MUC4, MUC5AC and MUC5B. Biochem Soc Trans 23: 800-805, 1995.
11. Shankar V, Pichan P, Eddy RL Jr, *et al*: Chromosomal localization of a human mucin gene (MUC8) and cloning of the cDNA corresponding to the carboxy terminus. Am J Respir Cell Mol Biol 16: 232-241, 1997.
12. Toribara NW, Roberton AM, Ho SB, *et al*: Human gastric mucin. Identification of a unique species by expression cloning. J Biol Chem 268: 5879-5885, 1993.
13. Williams SJ, Wreschner DH, Tran M, Eyre HJ, Sutherland GR and McGuckin MA: Muc13, a novel human cell surface mucin expressed by epithelial and hemopoietic cells. J Biol Chem 276: 18327-18336, 2001.
14. Yin BW and Lloyd KO: Molecular cloning of the CA125 ovarian cancer antigen: identification as a new mucin, MUC16. J Biol Chem 276: 27371-27375, 2001.
15. Bafna S, Singh AP, Moniaux N, Eudy JD, Meza JL and Batra SK: MUC4, a multifunctional transmembrane glycoprotein, induces oncogenic transformation of NIH3T3 mouse fibroblast cells. Cancer Res 68: 9231-9238, 2008.
16. Velcich A, Yang W, Heyer J, *et al*: Colorectal cancer in mice genetically deficient in the mucin Muc2. Science 295: 1726-1729, 2002.
17. Balague C, Gambus C, Carrato N, Porchet N, Aubert JP, Kim YS and Real FX: Altered expression of MUC2, MUC4, and MUC5 mucin genes in pancreas tissues and cancer cell lines. Gastroenterology 106: 1054-1061, 1994.
18. Voynow JA, Young LR, Wang Y, Horger T, Rose MC and Fischer BM: Neutrophil elastase increases MUC5AC mRNA and protein expression in respiratory epithelial cells. Am J Physiol 276: L835-L843, 1999.
19. Hovenberg HW, Davies JR and Carlstedt I: Different mucins are produced by the surface epithelium and the submucosa in human trachea: identification of MUC5AC as a major mucin from the goblet cells. Biochem J 318: 319-324, 1996.
20. Hovenberg HW, Davies JR, Herrmann A, Lindén CJ and Carlstedt I: MUC5AC, but not MUC2, is a prominent mucin in respiratory secretions. Glycoconj J 13: 839-847, 1996.
21. Sheehan JK, Brazeau C, Kutay S, Pigeon H, Kirkham S, Howard M and Thornton DJ: Physical characterization of the MUC5AC mucin: a highly oligomeric glycoprotein whether isolated from cell culture or *in vivo* from respiratory mucous secretions. Biochem J 347: 37-44, 2000.
22. Janek P, Briand P and Hartman NR: The effect of estrone-progesterone treatment on cell proliferation kinetics of hormone-dependent GR mouse mammary tumors. Cancer Res 35: 3698-3704, 1975.
23. Tsutsumida H, Swanson BJ, Singh PK, Caffrey TC, Kitajima S, Goto M, Yonezawa S and Hollingsworth MA: RNA interference suppression of MUC1 reduces the growth rate and metastatic phenotype of human pancreatic cancer cells. Clin Cancer Res 12: 2976-2987, 2006.
24. Chaturvedi P, Singh AP, Moniaux N, Senapati S, Chakraborty S, Meza JL and Batra SK: MUC4 mucin potentiates pancreatic tumor cell proliferation, survival, and invasive properties and interferes with its interaction to extracellular matrix proteins. Mol Cancer Res 5: 309-320, 2007.
25. Truant S, Bruyneel E, Gouyer V, De Wever O, Pruvot FR, Mareel M and Huet G: Requirement of both mucins and proteoglycans in cell-cell dissociation and invasiveness of colon carcinoma HT-29 cells. Int J Cancer 104: 683-694, 2003.
26. Ligtenberg MJL, Buijs F, Vos HL and Hilkens J: Suppression of cellular aggregation by high levels of episialin. Cancer Res 52: 2318-2324, 1992.
27. Duan R, Remeijer L, van Dun JM, Osterhaus AD and Verjans GM: Granulocyte macrophage colony-stimulating factor expression in human herpetic stromal keratitis: implications for the role of neutrophils in HSK. Inv Ophth Vis Sci 48: 277-284, 2007.
28. Tamamori Y, Sawada T, Nishihara T, *et al*: Granulocyte-colony stimulating factor enhances chimeric antibody K-MAC5 dependent cytotoxicity against pancreatic cancer mediated by polymorphonuclear neutrophils. Int J Oncol 21: 649-654, 2002.
29. Lieschke GJ and Burgess AW: Drug therapy: granulocyte colony-stimulating factor and granulocyte-macrophage colony-stimulating factor (1&2). N Engl J Med 327: 28-35, 99-106, 1992.
30. Stockmeyer B, Valerius T, Repp R, *et al*: Preclinical studies with FcγR bispecific antibodies and granulocyte colony-stimulating factor-primed neutrophils as effector cells against HER-2/neu overexpressing breast cancer. Cancer Res 57: 696-701, 1997.
31. Hinoda Y, Ikematsu Y, Horinochi M, *et al*: Increased expression of MUC1 in advanced pancreatic cancer. J Gastroenterol 38: 1162-1166, 2003.
32. Gimmi CD, Morrison BW, Mainprice BA, *et al*: Brest cancer associated antigen, DF3/MUC1, induces apoptosis of activated human T cells. Nat Med 2: 1367-1370, 1996.
33. Ho JJL: Mucins in the diagnosis and therapy of pancreatic cancer. Curr Pharm Des 6: 1881-1896, 2000.
34. Inaba T, Sano H, Kawahito Y, *et al*: Induction of cyclo-oxygenase-2 in monocyte/macrophage by mucins secreted from colon cancer cells. Proc Natl Acad Sci USA 100: 2736-2741, 2003.
35. Sugihara I, Yoshida M, Shigenobu T, *et al*: Different progression of tumor xenografts between mucin-producing and mucin-non-producing mammary adenocarcinoma-bearing mice. Cancer Res 66: 6175-6182, 2006.

J Toxicol Pathol 2011; 24: 25–36

Original

Enhanced Urinary Bladder, Liver and Colon Carcinogenesis in Zucker Diabetic Fatty Rats in a Multiorgan Carcinogenesis Bioassay: Evidence for Mechanisms Involving Activation of PI3K Signaling and Impairment of p53 on Urinary Bladder Carcinogenesis

Naomi Ishii[1], Min Wei[1], Anna Kakehashi[1], Kenichiro Doi[1], Shotaro Yamano[1], Masaaki Inaba[2], and Hideki Wanibuchi[1]

[1] Department of Pathology, Osaka City University Graduate School of Medicine, 1-4-3 Asahi-machi, Abeno-ku, Osaka 545-8585, Japan

[2] Department of Metabolism, Endocrinology and Molecular Medicine, Osaka City University Graduate School of Medicine, 1-4-3 Asahi-machi, Abeno-ku, Osaka 545-8585, Japan

Abstract: In the present study, modifying effects of diabetes on carcinogenesis induced in type 2 diabetes mellitus model Zucker diabetic fatty (ZDF) rats were investigated using a multiorgan carcinogenesis bioassay. Our results demonstrated enhancement of urinary bladder, colon and liver carcinogenesis in ZDF rats treated with five types of carcinogens (DMBDD). Elevated insulin and leptin and decreased adiponectin levels in the serum may be responsible for the high susceptibility of type 2 diabetes mellitus model rats to carcinogenesis in these organs. Possible mechanisms of increased susceptibility of diabetic rats to bladder carcinogenesis could be activation of the PI3K pathway and suppression of p53 in the urothelium in consequence of the above serum protein alterations. (DOI: 10.1293/tox.24.25; J Toxicol Pathol 2011; **24**: 25–36)

Key words: type 2 diabetes mellitus, bladder carcinogenesis, PI3K, p53

Introduction

Type 2 diabetes mellitus (T2DM) has been associated with a number of complications, such as cardiovascular disease, diabetic nephropathy and infection[1]. Recently, with the markedly improved survival of T2DM patients, attributed to the successful treatment of cardiovascular disease and infection control, the relationship between T2DM and cancer has been attracting attention. In epidemiological studies, T2DM was reported to be associated with increased risks of colon, pancreas, mammary, liver and urinary bladder cancers; however, the underlying mechanisms of increased cancer risks in T2DM patients remain unclear[2,3].

The influence of diabetes on carcinogenesis induced by chemical carcinogens has been investigated in the colon, stomach and mammary gland in experimental animals[4–6]. The number of colon tumors initiated by 1,2-dimethylhydrazine dihydrochloride (DMH) was increased in Otsuka Long-Evans Tokushima Fatty (OLETF) rats spontaneously developing T2DM compared with LETO rats, a non-diabetic strain[4]. Insulin resistance and hyperinsulinemia were suggested as direct risk factors for colon cancer[7]. Furthermore, db/db diabetic mice were reported to be highly susceptible to stomach carcinogenesis induced by *N*-methyl-*N*-nitrosourea (MNU), possibly in association with hyperinsulinemia and hyperleptinemia[5]. On the other hand, decreased susceptibility to MNU-induced mammary carcinogenesis was reported in streptozotocin-induced diabetic rats, possibly due to significantly lowered plasma levels of insulin and insulin-like growth factor 1 (IGF-1) during the promotion phase of carcinogenesis[6]. Based on these findings, metabolic abnormalities accompanying diabetes, such as hyperinsulinemia, hyperleptinemia and a high plasma level of IGF-1, have been proposed to play a role in cancer development in DM patients.

Zucker Diabetic Fatty (ZDF) rats closely mimic human adult onset T2DM and its related complications due to the inherited homozygous leptin receptor mutation, which leads to obesity and insulin resistance[8]. T2DM does not develop

Received: 15 September 2010, Accepted: 14 October 2010
Mailing address: Hideki Wanibuchi, Department of Pathology, Osaka City University Medical School, Asahi-machi 1-4-3, Abeno-ku, Osaka 545-8585, Japan.
TEL: 81-6-6645-3735 FAX: 81-6-6646-3093
E-mail: wani@med.osaka-cu.ac.jp

in lean littermate (Lean) animals[8]. ZDF animals show insulin resistance from the time of weaning but maintain normoglycemia until 8–10 weeks of age because of the compensatory hypersecretion of insulin[9]. ZDF rats develop overt diabetes and have defects in insulin secretion from around 8–10 weeks of age[10].

The purpose of the present study was to investigate the modifying effects of T2DM on carcinogenesis in diabetic ZDF rat using a multiorgan carcinogenesis bioassay. The multiorgan carcinogenesis bioassay uses treatment with five types of genotoxic carcinogens, namely *N*-diethylnitrosamine (DEN), MNU, *N*-butyl-*N*-(4-hydroxybutyl) nitrosamine (BBN), diisopropanolnitrosamine (DHPN) and DMH, with target organs including the liver, kidneys, urinary bladder, stomach, small intestine, colon, lungs and thyroid[11,12]. At the end of the experiment, histopathological analysis was performed to investigate cancer development. We also investigated the serum levels of several biologically active compounds, including insulin, leptin, adiponectin and IGF-1. Furthermore, to elucidate possible mechanisms underlying the modifying effects of T2DM, we analyzed alterations of the gene expression in the bladder urothelium in a 4-week BBN bladder carcinogenicity study.

Materials and methods

Animals

Five-week-old ZDF and control Lean rats were purchased from Charles River Laboratories Japan, Inc. (Kanagawa, Japan) and used after a 1-week acclimation period. They were housed in plastic cages (one rat/cage for ZDF rats, two rats/cage for Lean rats) in an environmentally-controlled room maintained at a temperature of 22 ± 2°C and relative humidity of 44 ± 5%, with a 12-h light/dark cycle and free access to water and food (MF pellet diet; Oriental Yeast Co., Ltd., Tokyo, Japan). Body weight and food intake were measured weekly during the experimental period. Water intake was measured three times a week in the first 4 weeks and once a week thereafter.

Chemicals

DEN, DMH and BBN were purchased from Tokyo Chemical Industry Co., Ltd. (Tokyo, Japan). MNU was purchased from Wako Pure Chemical Industries, Ltd. (Osaka, Japan), and DHPN was purchased from Nacalai Tesque Inc. (Kyoto, Japan).

Experimental protocol

Experimental protocols were approved by the Institution Animal Care and Use Committee of Osaka City University Medical School. The experimental protocol of the rat multiorgan carcinogenesis bioassay used in experiment 1 is shown in Fig. 1[11,12]. Twenty-six male ZDF rats at 6 weeks of age were divided randomly into two groups. Twenty ZDF rats were treated with five carcinogens, DEN, MNU, BBN, DMH and DHPN (DMBDD), as follows: a single i.p. injection of DEN (100 mg/kg b.w.) at the beginning of the experiment, followed by four i.p. injections of MNU (20 mg/kg b.w.) from week 1 to 2, and four s.c. injections of DMH (40 mg/kg b.w.) from week 3 to 4. Also, 0.05% BBN in drinking water was administered to rats for two weeks from commencement of the experiment, and then DHPN in drinking water was administered to the rats for the following 2 weeks. Six control ZDF rats were administered tap water and received vehicle injections (0.9% saline) in the same manner. Twenty-seven male Lean rats at 6 weeks of age were divided randomly into two groups and treated with DMBDD (20 rats) and vehicle (7 rats), respectively, as described above. DHPN was administered to Lean rats at a concentration of 0.1% in drinking water. As ZDF rats were drinking more water than Lean rats from week 3 to 4, the concentrations of DHPN administered to the ZDF rats were diluted to give the same amount of DHPN per b.w. as the Lean rats based on their body weight and water intake. After the initiation treatments, all rats were maintained without any treatment until the end of the study. Blood glucose was examined weekly from week 3 to 7 and once every two weeks from week 8 to 30 via the tail vein using a blood glucose test meter (Glutest Ace R; Sanwa Kagaku Kenkyusho Co., Ltd., Nagoya, Japan). At the end of week 30, all surviving animals were euthanized under deep anesthesia, target organs were taken out and the liver, kidney and spleen weights were measured. All target organs were fixed in 10% phosphate-buffered formalin and embedded in paraffin for histopathological examination. Blood serum was collected for biochemical analyses. Part of the liver tissues was snap frozen in liquid nitrogen and stored at −80°C.

In experiment 2, 12, 6-week-old male ZDF or Lean rats were divided randomly into two groups each. BBN in drinking water was administered for 4 weeks from commencement of the experiment to ZDF (6) or Lean (6) rats. The remaining 6 ZDF and 6 Lean rats were administered tap water. Given the differences in water intake and body weight between the ZDF and Leans rats, water intake and body weights were measured three times a week, and the BBN concentration was adjusted to give the same amount of BBN per b.w. to both strains of rats based on the water intake per body weight per day from commencement of the experiment. Briefly, 0.05% BBN was administered to the strain of rats drinking less water (g/kg, b.w.), and the concentration of BBN was diluted and administered to the strain of rats drinking more water. Blood glucose was examined weekly from week 1 to 4. At week 4, all rats were euthanized under deep anesthesia, and blood serum was collected for biochemical analyses. The bladder mucosa was harvested using the method described previously[13]. Part of the liver tissues was snap frozen in liquid nitrogen and stored at −80°C.

Blood biochemistry analysis

Blood biochemistry was analyzed at the end of the experiments (week 30 in experiment 1 and week 4 in experiment 2) by Mitsubishi Chemical Medience Corporation (Tokyo, Japan). The serum levels of insulin, leptin, adiponectin, IGF-1, tumor necrosis factor α (TNFα) and inter-

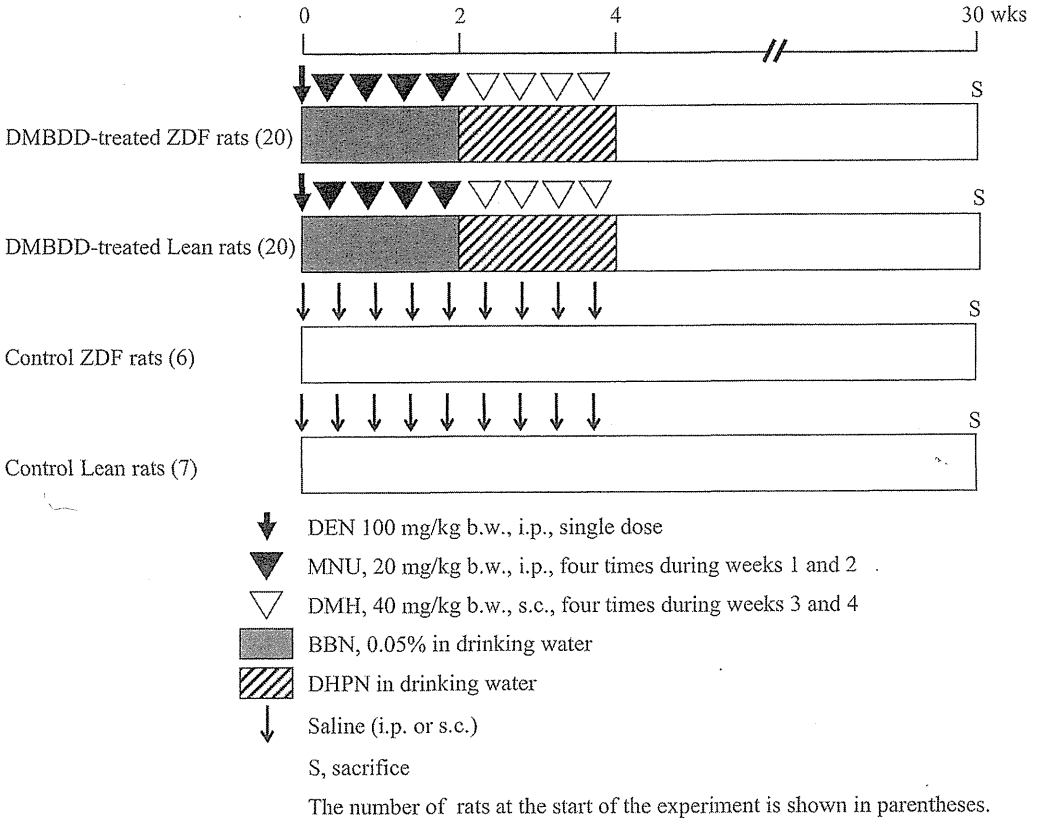

Fig. 1. Experimental protocol of experiment 1 (DMBDD model).

leukin-6 (IL-6) of all surviving rats were measured using rat ELISA kits (insulin, Shibayagi Co., Ltd., Gunma, Japan; leptin, Morinaga Institute of Biological Science, Inc., Kanagawa, Japan; adiponectin, Otsuka Pharmaceutical Co., Ltd., Tokyo, Japan; IGF-1, TNFα and IL-6, R&D Systems, Inc., Minneapolis, MN, USA) according to the manufacturers' instructions.

RNA preparation and real-time quantitative PCR

RNA from the bladder mucosa and liver was isolated using TRIZOL Reagent (Life Technologies Japan Ltd., Tokyo, Japan) according to the manufacturer's instructions. Synthesis of cDNA was performed with 600 ng RNA using an Advantage RT-for-PCR kit (Takara Bio, Inc., Shiga, Japan). Real-time quantitative PCRs for phosphatidylinositol 3-kinase (PI3K), p53, PCNA and β-actin as an internal control for the bladder mucosa and IGF-1 and rsp18 as an internal control for the liver were performed using an Applied Biosystems 7500 Fast Real-Time PCR System (Applied Biosystems, Inc., Tokyo, Japan) as described previously[13,14]. Briefly, 20 μl containing 1 μl of the respective TaqMan Gene Expression Assays (Applied Biosystems, Inc., Tokyo, Japan), 10 μl TaqMan Fast Universal PCR Master Mix (Applied Biosystems, Inc., Tokyo, Japan) and 5 μl diluted cDNA were applied to a Fast 96-well Reaction Plate.

Serially diluted standard cDNA was included in each TaqMan PCR reaction to create standard curves. The amounts of gene products in the test samples were estimated relative to the respective standard curves. Values for target genes were normalized to those for β-actin or rsp18.

Statistical analysis

All mean values are reported as means ± SD. Statistical analyses were performed using the StatLight program (Yukms Co., Ltd., Tokyo, Japan). Homogeneity of variance analysis was performed by the F test. Differences in mean values between the control and carcinogen-treated groups were evaluated by Student's *t*-test when the variance was homogeneous and Welch's *t*-test when the variance was heterogeneous. Incidence was assessed by Fisher's exact probability test. *P* values less than 0.05 were considered significant.

Results

General observations

Experiment 1: Five DMBDD-treated ZDF rats were found dead or moribund at weeks 17, 21, 22, 27 and 29. Furthermore, two control ZDF rats were found dead or moribund without any discernible cause at weeks 21 and 26. All DMBDD-treated and control Lean rats were alive at the end of the study. As bladder, small intestine and liver tumors

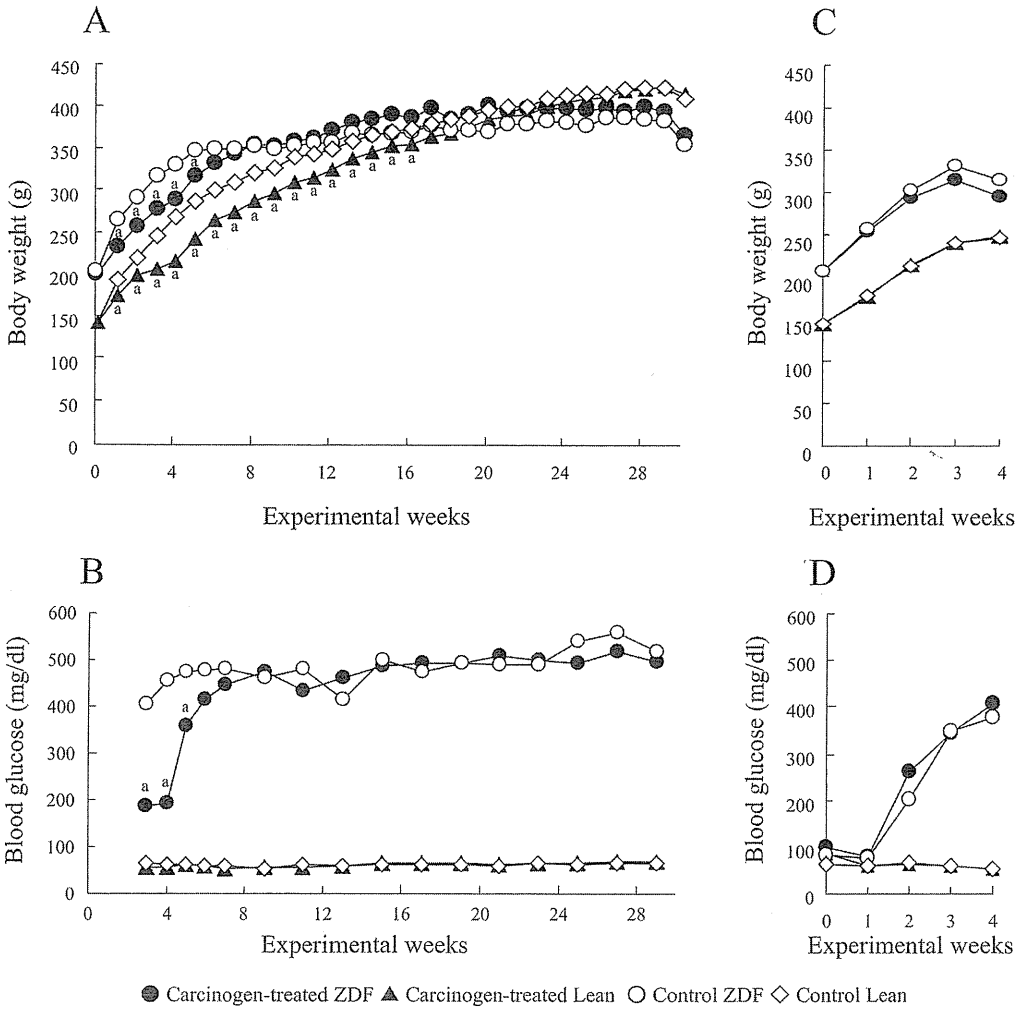

Fig. 2. Time course of body weight and blood glucose level in experiment 1 (A, B) and experiment 2 (C, D).
[a] $P<0.05$ vs. control rats of the same genotype.

were found in the DMBDD-treated ZDF rat that died at week 17, all rats were included in the effective animals for histopathological analysis.

Body weight curves, final body weight and absolute and relative organ weights of the rats in experiment 1 are shown in Fig. 2A and Table 1. The body weights of both the DMBDD-treated ZDF and Lean rats were significantly decreased during administration of DMBDD compared with the control rats of the same genotype; however, the final body weights of both the ZDF and Lean rats administered DMBDD were not significantly changed as compared with the control rats of the same genotype. The body weights of the ZDF rats were significantly higher during the DMBDD treatment period but were significantly lower than those of the Lean rats at the end of the study irrespective of whether or not they received carcinogen treatment.

During BBN treatment (weeks 1 and 2), the total BBN intake of the ZDF rats (0.54 ± 0.07 mg/kg b.w.) was significantly lower than that of the Lean rats (0.63 ± 0.04 mg/kg b.w.). During DHPN treatment (weeks 3 and 4), almost the same total amount of DHPN was given to both strain rats (1.3 ± 0.4 mg/kg b.w. for the ZDF rats and 1.3 ± 0.1 mg/kg b.w. for the Lean rats) by adjusting the concentration of DHPN based on the water intake and body weight, as described in the Methods.

DMBDD administration inhibited food intake of both the ZDF and Lean rats compared with the control rats of the same genotype. Food intake was significantly increased in the DMBDD-treated and non-treated ZDF rats when compared with the Lean rats receiving the same treatment throughout the experiment (data not shown).

The absolute liver and spleen weights and relative spleen weight of the DMBDD-treated ZDF rats were significantly higher than those of the control ZDF rats. Furthermore, the absolute and relative spleen weights in the DMBDD-treated Lean group were significantly elevated compared with those of the Lean control animals.

Experiment 2: All rats survived to the end of the study.

Table 1. Final Body and Organ Weights (Experiment 1)

	DMBDD		Control	
	ZDF	Lean	ZDF	Lean
Initial no. of rats	20	20	6	7
Final no. of rats	15	20	4	7
Survival rate (%)	75	100	67	100
Final body weight (g)	367 ± 19	416 ± 24	355 ± 41	411 ± 32
Absolute (g)				
Liver	18.0 ± 2.4[a]	10.6 ± 0.9	15.0 ± 3.8	10.9 ± 0.9
Kidneys	4.4 ± 2.7	2.3 ± 0.1	3.6 ± 0.3	2.2 ± 0.2
Spleen	0.9 ± 0.5[a]	0.6 ± 0.1[a]	0.4 ± 0.2	0.5 ± 0.0
Relative (g/100g bw)				
Liver	4.9 ± 0.6	2.5 ± 0.1[a]	4.4 ± 0.9	2.7 ± 0.1
Kidneys	1.2 ± 0.7	0.5 ± 0.0	1.1 ± 0.1	0.5 ± 0.0
Spleen	0.2 ± 0.2[a]	0.2 ± 0.0[a]	0.1 ± 0.0	0.1 ± 0.0

[a] $P<0.05$ vs. control rats of the same genotype.

Table 2. Blood Biochemistry

Experiment 1	DMBDD		Control	
week 30	ZDF	Lean	ZDF	Lean
HbA1c (%)	8.3 ± 0.7*, [a]	3.3 ± 0.1	9.6 ± 0.5*	3.3 ± 0.1
Glucose (mg/dl)	479 ± 45*	137 ± 22	512 ± 51*	129 ± 8
T-Cho (mg/dl)	241 ± 69*, [a]	92 ± 19	404 ± 98*	92 ± 10
TG (mg/dl)	740 ± 353*	51 ± 14	1053 ± 404*	61 ± 10
AST (IU/l)	390 ± 222*	159 ± 38	618 ± 208*	148 ± 35
ALT (IU/l)	428 ± 265*, [a]	61 ± 51[a]	783 ± 353*	32 ± 3
γ-GTP (IU/l)	27 ± 15*, [a]	2 ± 1[a]	72 ± 28*	1 ± 0
Experiment 2	BBN		Control	
week 4	ZDF	Lean	ZDF	Lean
HbA1c (%)	5.8 ± 0.6*	3.2 ± 0.0	5.6 ± 0.6*	3.2 ± 0.0
Glucose (mg/dl)	311 ± 62*	93 ± 21	261 ± 86*	102 ± 6
T-Cho (mg/dl)	99 ± 12*	66 ± 5	97 ± 9*	71 ± 4
TG (mg/dl)	304 ± 127*	26 ± 7	377 ± 119*	24 ± 6
AST (IU/l)	454 ± 331	170 ± 16	351 ± 177*	152 ± 20
ALT (IU/l)	333 ± 319	38 ± 3	234 ± 171*	39 ± 4
γ-GTP (IU/l)	6 ± 5	2 ± 1	4 ± 1*	2 ± 0

* $P<0.05$ vs. Lean rats receiving the same treatment. [a] $P<0.05$ vs. control rats of the same genotype. HbA1c, hemoglobin A1c; T-Cho, total cholesterol; TG, triglyceride; AST, aspartate aminotransferase; ALT, alanine aminotransferase; γ-GTP, γ-glutamyl transpeptidase.

Body weight curves are shown in Fig. 2C. The average body weights of the ZDF rats were significantly higher than those of the Lean rats throughout the experiment. BBN treatment had no effect on the body weights of the ZDF and Lean rats. There was no significant difference in the total intake of BBN between ZDF (1.4 ± 0.5 mg/kg b.w.) and Lean rats (1.1 ± 0.0 mg/kg b.w.).

Time course changes of blood glucose level

Time course changes of the blood glucose level in experiments 1 and 2 are shown in Fig. 2B and D, respectively.

In experiment 1, the blood glucose levels were significantly higher in the DMBDD-treated and control ZDF rats throughout the experimental period compared with the Lean rats receiving the same treatment, respectively. The level of blood glucose was significantly suppressed only in the DMBDD-treated ZDF rats compared with the control ZDF rats at weeks 3–5, possibly due to the significant decrease of food intake during weeks 1–5 caused by DMBDD treatment.

In experiment 2, the blood glucose levels of the BBN-initiated and control ZDF rats were significantly elevated compared with the Lean rats receiving the same treatment from week 2 to 4; however, BBN treatment had no effect on the blood glucose level in the ZDF and Lean rats.

Blood biochemistry

The results of the blood biochemistry analysis in experiments 1 and 2 are shown in Table 2.

In experiment 1, the level of hemoglobin A1c (HbA1c),

Table 3. Histopathological Findings (Experiment 1)

Site and type of lesion		Incidence (%)				Multiplicity (No./rat)			
		DMBDD		Control		DMBDD		Control	
		ZDF	Lean	ZDF	Lean	ZDF	Lean	ZDF	Lean
Effective no. of rats [b]		20	20	6	7	20	20	6	7
Urinary bladder	Simple hyperplasia	19 (95)[a]	14 (70)[a]	0 (0)	0 (0)	-	-	-	-
	PN hyperplasia	9 (45)	6 (30)	0 (0)	0 (0)	1.0 ± 1.3[a]	0.4 ± 0.7[a]	0	0
	Papilloma	4 (20)	4 (20)	0 (0)	0 (0)	0.3 ± 0.7	0.3 ± 0.6	0	0
	TCC	11 (55)*, [a]	1 (5)	0 (0)	0 (0)	0.7 ± 0.8*, [a]	0.1 ± 0.2	0	0
	Total tumors [c]	14 (70)*, [a]	5 (25)	0 (0)	0 (0)	1.0 ± 0.9*, [a]	0.3 ± 0.6[a]	0	0
Colon	Adenoma	1 (5)	0 (0)	0 (0)	0 (0)	0.1 ± 0.2	0	0	0
	Adenocarcinoma	10 (50)*	3 (15)	0 (0)	0 (0)	0.8 ± 0.9*, [a]	0.2 ± 0.5	0	0
	Mucinous carcinoma	3 (15)	1 (5)	0 (0)	0 (0)	0.2 ± 0.4	0.1 ± 0.2	0	0
	Total tumors	12 (60)*, [a]	4 (20)	0 (0)	0 (0)	1.0 ± 1.0*, [a]	0.3 ± 0.6	0	0
Small intestine	Adenocarcinoma	9 (45)*	0 (0)	0 (0)	0 (0)	0.7 ± 1.0*	0	0	0
	Mucinous carcinoma	1 (5)	0 (0)	0 (0)	0 (0)	0.1 ± 0.2	0	0	0
	Total tumors	10 (50)*	0 (0)	0 (0)	0 (0)	0.8 ± 1.0*, [a]	0	0	0
Liver	Adenoma	8 (40)*	1 (5)	0 (0)	0 (0)	0.6 ± 0.8*, [a]	0.1 ± 0.2	0	0
Kidney	Adenoma	4 (20)	7 (35)	0 (0)	0 (0)	0.2 ± 0.4[a]	0.5 ± 0.7[a]	0	0
	Mesenchymal tumor	5 (25)	2 (10)	0 (0)	0 (0)	0.3 ± 0.4[a]	0.1 ± 0.3	0	0
	Nephroblastoma	9 (45)	3 (15)	0 (0)	0 (0)	0.7 ± 0.9*, [a]	0.2 ± 0.4	0	0
	TCC	2 (10)	0 (0)	0 (0)	0 (0)	0.2 ± 0.5	0	0	0
	Total tumors	12 (60)[a]	9 (45)	0 (0)	0 (0)	1.3 ± 1.2[a]	0.7 ± 0.9[a]	0	0
Lung	Adenoma	5 (25)*	20 (100)[a]	0 (0)	0 (0)	0.4 ± 0.7*, [a]	3.7 ± 2.0[a]	0	0
	Carcinoma	3 (15)	3 (15)	0 (0)	0 (0)	0.2 ± 0.5	0.3 ± 0.8	0	0
	Total tumors	7 (35)*	20 (100)[a]	0 (0)	0 (0)	0.6 ± 0.8*, [a]	4.0 ± 2.4[a]	0	0
Thyroid gland	Follicular adenoma	1 (5)	2 (10)	0 (0)	0 (0)	0.1 ± 0.4	0.1 ± 0.3	0	0
	Follicular carcinoma	0 (0)*	5 (25)	0 (0)	0 (0)	0*	0.3 ± 0.4[a]	0	0
	Total tumors	1 (5)*	7 (35)	0 (0)	0 (0)	0.1 ± 0.4	0.4 ± 0.5[a]	0	0
Esophagus	Papilloma	3 (15)	0 (0)	0 (0)	0 (0)	0.2 ± 0.4	0	0	0
Forestomach	SCC	1 (5)	0 (0)	0 (0)	0 (0)	0.1 ± 0.2	0	0	0

* $P<0.05$ vs. Lean rats receiving the same treatment. [a] $P<0.05$ vs. control rats of the same genotype. PN, papillary or nodular; TCC, transitional cell carcinoma; SCC, squamous cell carcinoma. [b] Number of rats found dead or moribund from week 17 to 30. [c] Papilloma + TCC.

one of the characteristics of diabetes, was significantly higher in both the DMBDD-treated and control ZDF animals than in the Lean rats receiving the same treatment. Furthermore, the total cholesterol (T-Cho) and triglyceride (TG) levels were also significantly increased in the DMBDD-administered and control ZDF rats but not in the Lean rats receiving the same treatment.

In experiment 2, the levels of HbA1c, T-Cho and TG were significantly higher in both the BBN-treated and control ZDF rats than in the Lean rats receiving the same treatment. Moreover, no influence of BBN treatment was apparent on HbA1c, T-Cho and TG in both the ZDF and Lean rats.

Histopathological findings in experiment 1

Table 3 summarizes the data on the incidence and multiplicity of preneoplastic and neoplastic lesions induced by DMBDD administration. No tumors were found in the control ZDF and Lean rats. Macroscopically, several very large tumors occupying the whole urinary bladder were found in the DMBDD-treated ZDF rats but not in the Lean rats (Fig. 3). Histological examination demonstrated significant elevation of the incidences and multiplicities of transitional ce carcinomas (TCC: 55%, 0.7 ± 0.8/rat) and total tumors (pa illoma +TCC: 70%, 1.0 ± 0.9/rat) in the DMBDD-admini tered ZDF animals as compared with the DMBDD-initiate Lean rats (TCC, 5% and 0.1 ± 0.2/rat; total tumors, 25% a 0.3 ± 0.6/rat).

The incidences and multiplicities of colon adenocarc noma and total colon tumors (adenocarcinoma, 50% and 0 ± 0.9/rat; total tumors, 60% and 1.0 ± 1.0/rat) were signi cantly increased in the DMBDD-treated ZDF rats as co pared with the DMBDD-treated Lean rats (adenocarcinom 15% and 0.2 ± 0.5/rat; total tumors, 20% and 0.3 ± 0.6/ra Furthermore, the incidences and multiplicities of small i testine adenocarcinoma and total tumors were significant higher in the DMBDD-administered ZDF rats (adenocarc noma, 45% and 0.7 ± 1.0/rat; total tumors, 50% and 0.8 1.0/rat) than in the DMBDD-treated Lean animals (no tum was found).

The incidence and multiplicity of hepatocellular a enoma were significantly increased in the DMBDD-treat ZDF rats (40%, 0.6 ± 0.8/rat) compared with the DMBDI

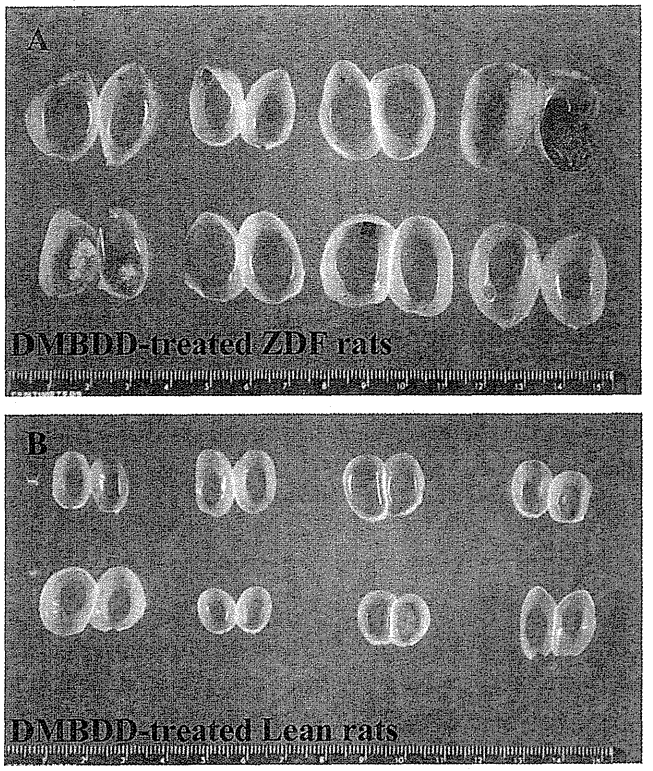

Fig. 3. Macroscopic view of the urinary bladder in experiment 1. A: DMBDD-treated ZDF rats. B: DMBDD-treated Lean rats.

treated Lean group (5%, 0.1 ± 0.2/rat). No hepatocellular carcinomas were found in the DMBDD-initiated ZDF and Lean rats.

No renal cell carcinoma was observed in any groups. There were no significant differences in renal cell adenoma between the DMBDD-treated ZDF and Lean rats. The multiplicity of nephroblastoma in the DMBDD-treated ZDF rats (0.7 ± 0.9/rat) was significantly increased compared with the DMBDD-administered Lean animals (0.2 ± 0.4/rat).

On the other hand, the incidences and multiplicities of adenoma and total tumors in lung and thyroid follicular carcinoma were significantly decreased in the DMBDD-treated ZDF rats compared with the DMBDD-initiated Lean group.

Serum levels of insulin, leptin, adiponectin and IGF-1

In experiment 1, the serum insulin level in the DMBDD-treated ZDF rats was significantly higher than in the treated Lean groups (Fig. 4A, $P<0.001$). Furthermore, a significant increase in serum leptin level was found in the ZDF rats compared with the Lean rats receiving the same treatment (Fig 4C; DMBDD-treated, $P<0.0001$; control, $P<0.05$). Moreover, there was a significant decrease in the serum adiponectin level in the ZDF rats compared with the Lean rats receiving the same treatment (Fig. 4E; DMBDD-treated, $P<0.0001$; control, $P<0.05$). In contrast to our expectation, the serum levels of IGF-1 of the DMBDD-treated and control ZDF rats were significantly decreased compared with the Lean rats receiving the same treatment (Fig. 4G; DMBDD-treated, $P<0.0001$; control, $P<0.0001$).

In experiment 2, the serum insulin level was significantly increased in the BBN-treated and control ZDF rats compared with the Lean rats receiving the same treatment (Fig. 4B; BBN-treated, $P<0.0001$; control, $P<0.0001$). Similarly, the serum leptin level in the ZDF rats was significantly increased compared with the Lean rats receiving the same treatment (Fig. 4D; BBN-treated, $P<0.0001$; control, $P<0.0001$); however, no significant differences were apparent in the serum level of adiponectin and IGF-1 (Fig. 4F and H).

The TNFα and IL-6 serum levels were under the limit of detection.

IGF-1 mRNA expression in the liver

Since there was no increase of the IGF-1 level in the serum of ZDF rats at weeks 4 and 30, its mRNA expression level was examined in the liver, which is the main organ in which IGF-1 is produced. IGF-1 mRNA expression was inhibited in the liver of the DMBDD-treated and control ZDF rats compared with the Lean rats receiving the same treatment at week 30 in experiment 1 but without significance (Fig. 5A). Furthermore, there was a significant decrease of IGF-1 mRNA expression in the BBN-treated and control ZDF rats compared with the Lean rats receiving the same treatment at week 4 in experiment 2 (Fig. 5B; BBN-treated, $P<0.05$; control, $P<0.001$).

PI3K, p53 and PCNA mRNA expression in the bladder epithelium of BBN-treated rats (experiment 2)

Since alterations of the serum levels of insulin, leptin and adiponectin were observed, we further investigated the downstream effector molecules of these receptors.

Significant increases of PI3K mRNA expression in the bladder epithelium of the BBN-initiated and control ZDF rats were found compared with the Lean rats receiving the same treatment (Fig. 6A; BBN-treated, $P<0.0001$; control, $P<0.001$).

Four-week treatment with BBN significantly decreased the p53 mRNA expression level in the urothelium of the ZDF rats but had no effect on the Lean rats (Fig. 6B, $P<0.001$). Furthermore, p53 mRNA expression was significantly inhibited in the BBN-treated ZDF rats compared with the treated Lean animals (Fig. 6B, $P<0.05$).

The expression of mRNA of PCNA, which is a marker for cell proliferation, was significantly increased in the BBN-treated ZDF rats compared with the control ZDF animals (Fig. 6C, $P<0.05$) and showed a tendency to increase as compared with the BBN-treated Lean rats.

Discussion

The present study demonstrated enhancement effects of T2DM on urinary bladder, colon and liver carcinogenesis in ZDF type 2 diabetes rats, indicating the high multiorgan carcinogenic susceptibility of this strain of rats. In epidemiological studies, T2DM was reported to be associated with